Measuring the masses and spins of astrophysical black holes

Łukasz Stawarz
Astronomical Observatory of the Jagiellonian University

Zakopane, 21.06.2019

NATURE ASTRONOMY | VOL 3 | JANUARY 2019 | 1 | www.nature.com/natureastronomy

editorial

Cosmic celebrities with gravitas

Black holes have the distinct honour of being the most popular and potentially the least well-understood objects in the Universe. This issue's Insight explores how far black hole research has come since its inception, though it still has a long way to go.

Since 1784, when John Michell first thought of the concept of an object so heavy that even light cannot escape its gravitational pull, black holes have fascinated, puzzled and even terrified the public and scientists alike. It was Albert Einstein, with his foundational theory of general relativity (GR), and Karl Schwarzschild, who found the corresponding solution to GR's equations, that placed black holes on a proper physical footing in 1915. In the following century, black holes became a topic of intense scientific research, while at the same time entering the mainstream collective consciousness as one of the staples of the sci-fi genre (with milestones like the dubious 1979 Disney movie *The Black Hole* and the more acclaimed 2014 *Interstellar*). Key observational discoveries, like the orbits of stars around Sgr A*, quasars and the recent directly probed by classical Newtonian dynamics at scales significantly larger than its Schwarzschild radius. But while such dynamical considerations are only possible for those black holes closest to us (like the one at the centre of M87), we have to rely on much rougher estimates when looking at black holes in most other galaxies.

Given their fundamental importance, understanding how black holes grow their mass is key in constraining their formation and evolution and how their growth might impact the growth of their host galaxies (see the News & Views in this issue and our focu issue last March). In the Insight, Thaisa Storchi-Bergmann and Allan Schnorr-Müller review how supermassive black holes are fed, while Marianne Vestergaard discusses current problems and open issues with calculating masses of black holes in other galaxies.

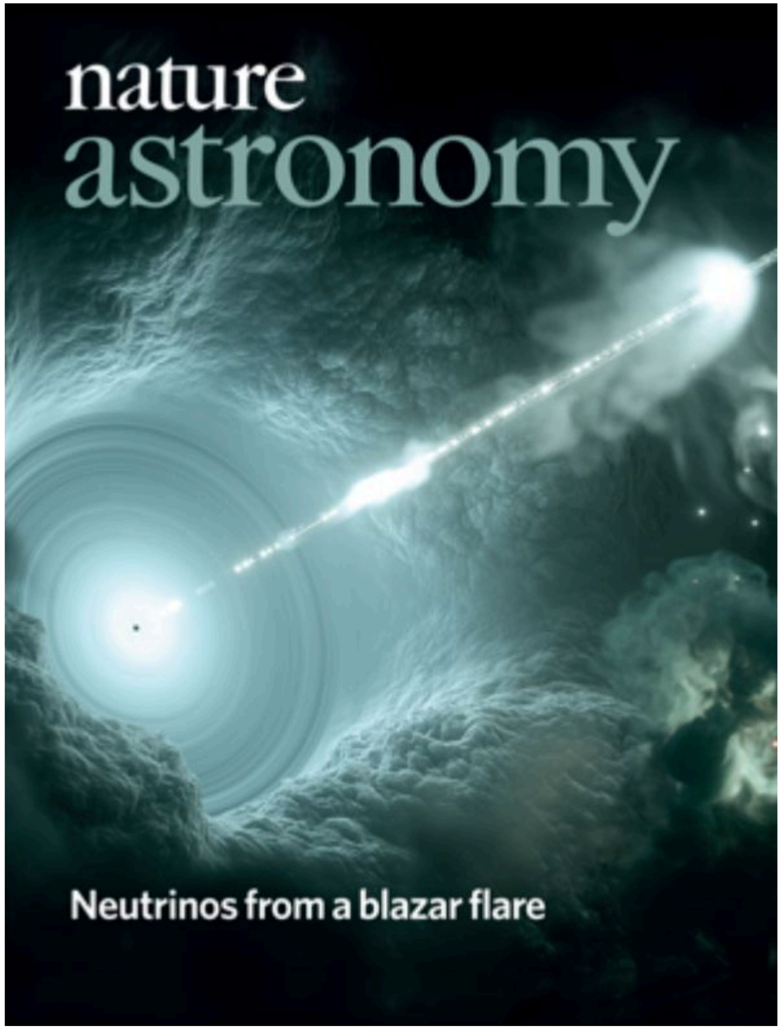

- **no-hair theorem/conjecture:** black holes can be completely characterized by only three externally observable classical parameters: **mass**, electric charge, and **angular momentum (spin)**. All other information (for which "hair" is a metaphor) about the matter which formed a black hole or is falling into it, "disappears" behind the black-hole event horizon and is therefore permanently inaccessible to external observers (J.A. Wheeler: “black holes have no hair”)

- how exactly can we *“**observe**”* black holes in the Universe? how can we measure their masses and spins?

- **this talk:** black holes as astrophysical objects, interacting with their environment (gravitational potential, but also jets/outflows), and thus ***observable***

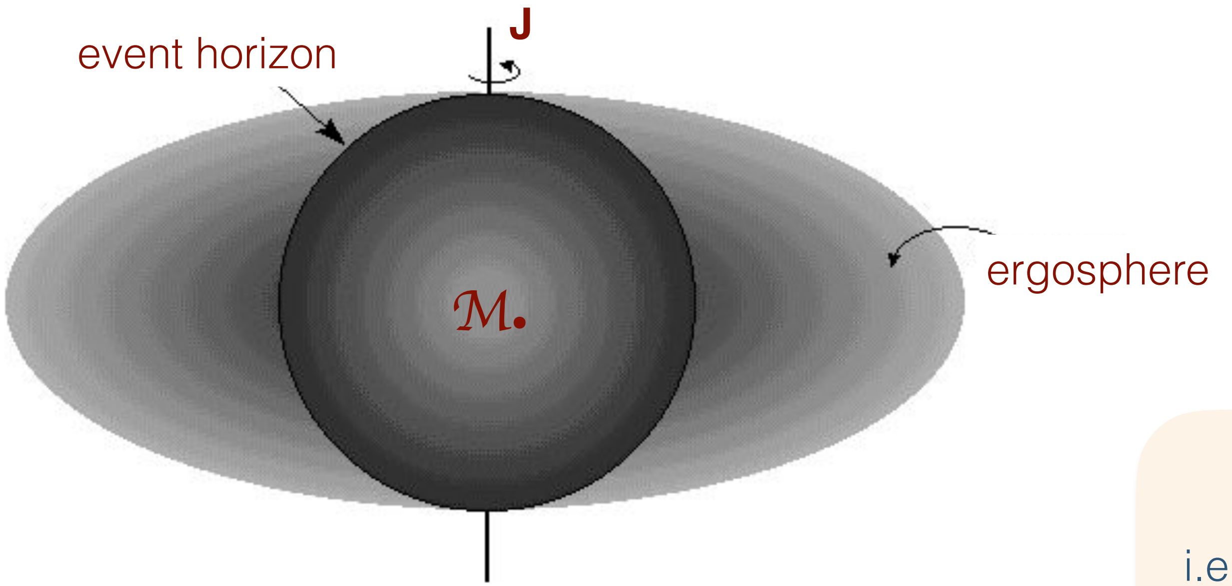

gravitational radius,
i.e. mass expressed in length units

$$r_{\rm g} = \frac{G\mathcal{M}_\bullet}{c^2} \approx \left(\frac{\mathcal{M}_\bullet}{M_\odot}\right)\,\text{km}$$

$$M_\odot = 2 \times 10^{30}\,\text{kg}$$

angular momentum (spin)
expressed in length units

$$a = \frac{J}{c\,\mathcal{M}_\bullet}$$

$$J_{\rm max} = \frac{G\mathcal{M}_\bullet^2}{c}$$

$$0 \quad \leq \quad a_\star \equiv \frac{a}{r_{\rm g}} \quad \leq \quad 1$$

event horizon (Schwarzchild radius) r_S
and static limit r_C

$$r_{\rm S} = r_{\rm g} + \sqrt{r_{\rm g}^2 - a^2}$$

$$r_{\rm C} = r_{\rm g} + \sqrt{r_{\rm g}^2 - a^2 \cos^2\theta}$$

- charged BH are expected to neutralize quickly by attracting charge of the opposite sign
- J_{max} as you cannot have a "naked singularity", i.e. a singularity exposed to the rest of the Universe
- **Lense-Thirring/frame-dragging effect**: due to the twisting of a spacetime by rotating BH, an object within the ergosphere cannot appear stationary with respect to an outside observer
- **Penrose process**: since the ergosphere is outside the event horizon, it is still possible for an object that enters that region to escape from the gravitational pull of the BH, possibly removing the BH rotational energy ("reducible mass", although note that the gravitational mass of the BH has to increase at the same time)
- **Blandford–Znajek process**: the BH rotational energy and angular momentum transported electromagnetically outwards (**jets!**) due to the magnetic field supported within the ergosphere by the accreting matter

$$\frac{E_{\rm rot}}{\mathcal{M}_\bullet c^2} = 1 - \sqrt{\frac{1}{2} + \frac{1}{2}\sqrt{1 - \left(\frac{a}{r_{\rm g}}\right)^2}} \leq 0.3$$

the innermost stable circular orbit: r_{ISCO}

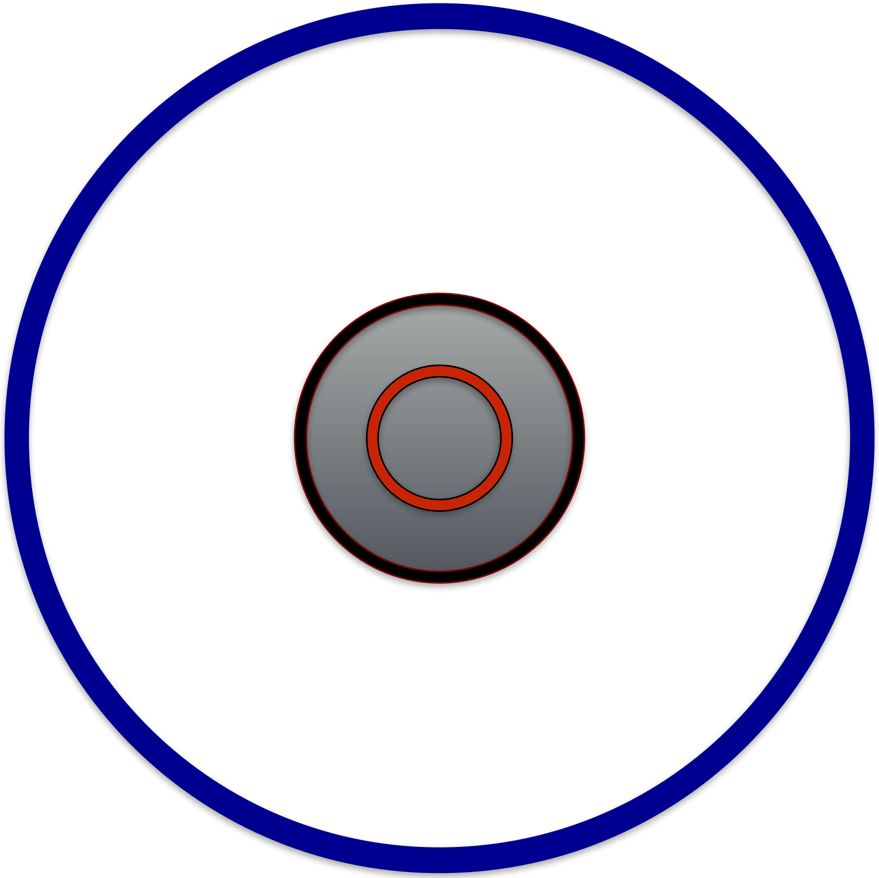

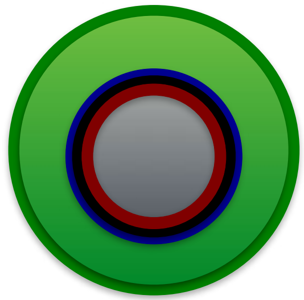

non-spinning BH: **a=0**

$r_g = GM/c^2$

$r_S = 2\ r_g$

$r_{ISCO} = 6\ r_g$

maximally-spinning BH: **a~1**

$r_g = GM/c^2$

$r_S \sim r_g$

$r_C(\pi/2) \sim 2\ r_g$

$r_{ISCO} \sim r_g$

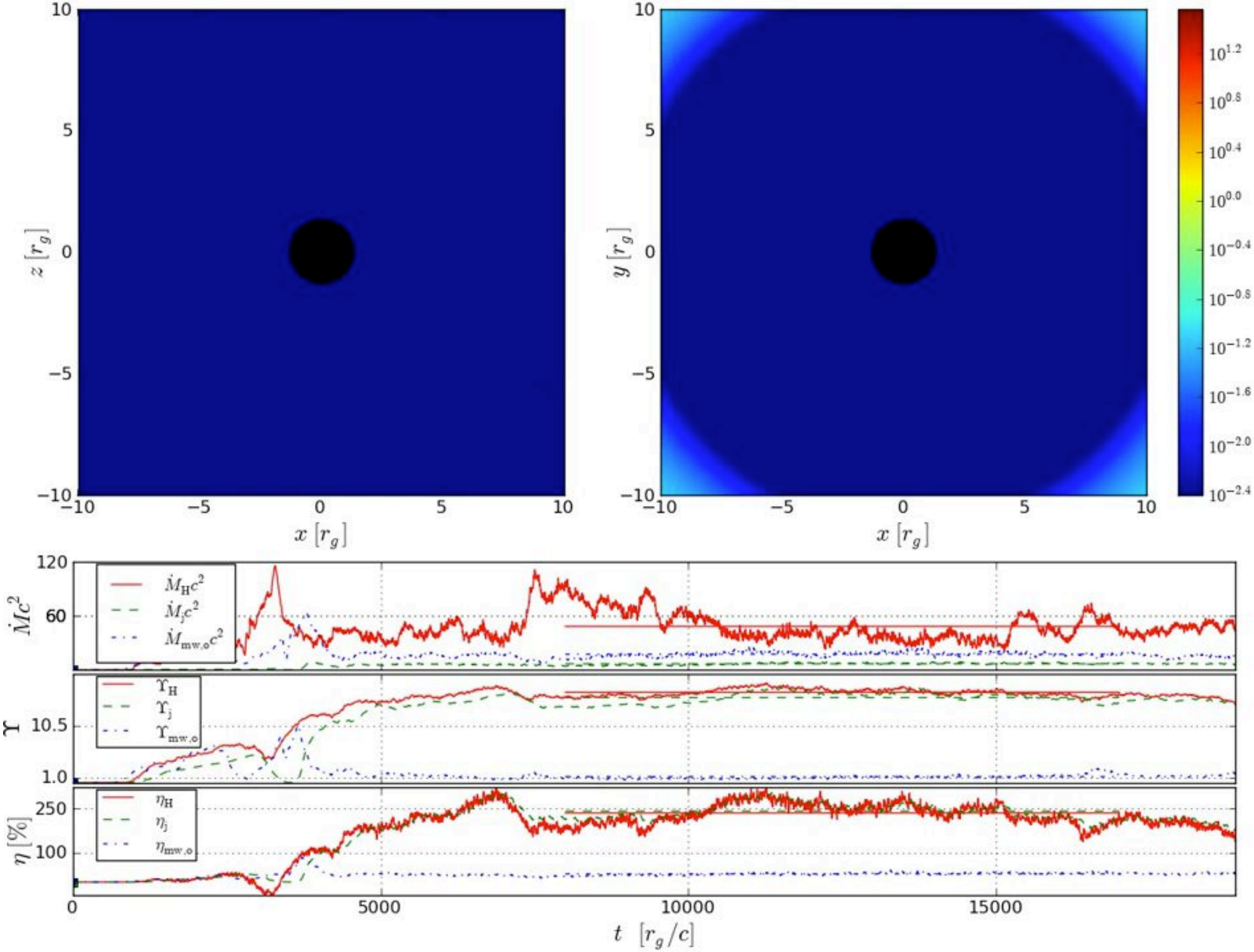

McKinney et al. 2012: log of rest-mass density in colour in both the *z*–*x* plane at *y* = 0 (top left-hand panel) and the *y*–*x* plane at *z* = 0 (top right-hand panel). The black lines trace field lines, where the thicker black lines show where field is lightly mass-loaded. Panels below: accretion rate, the horizon's dimensionless magnetic flux, and the jet production efficiency

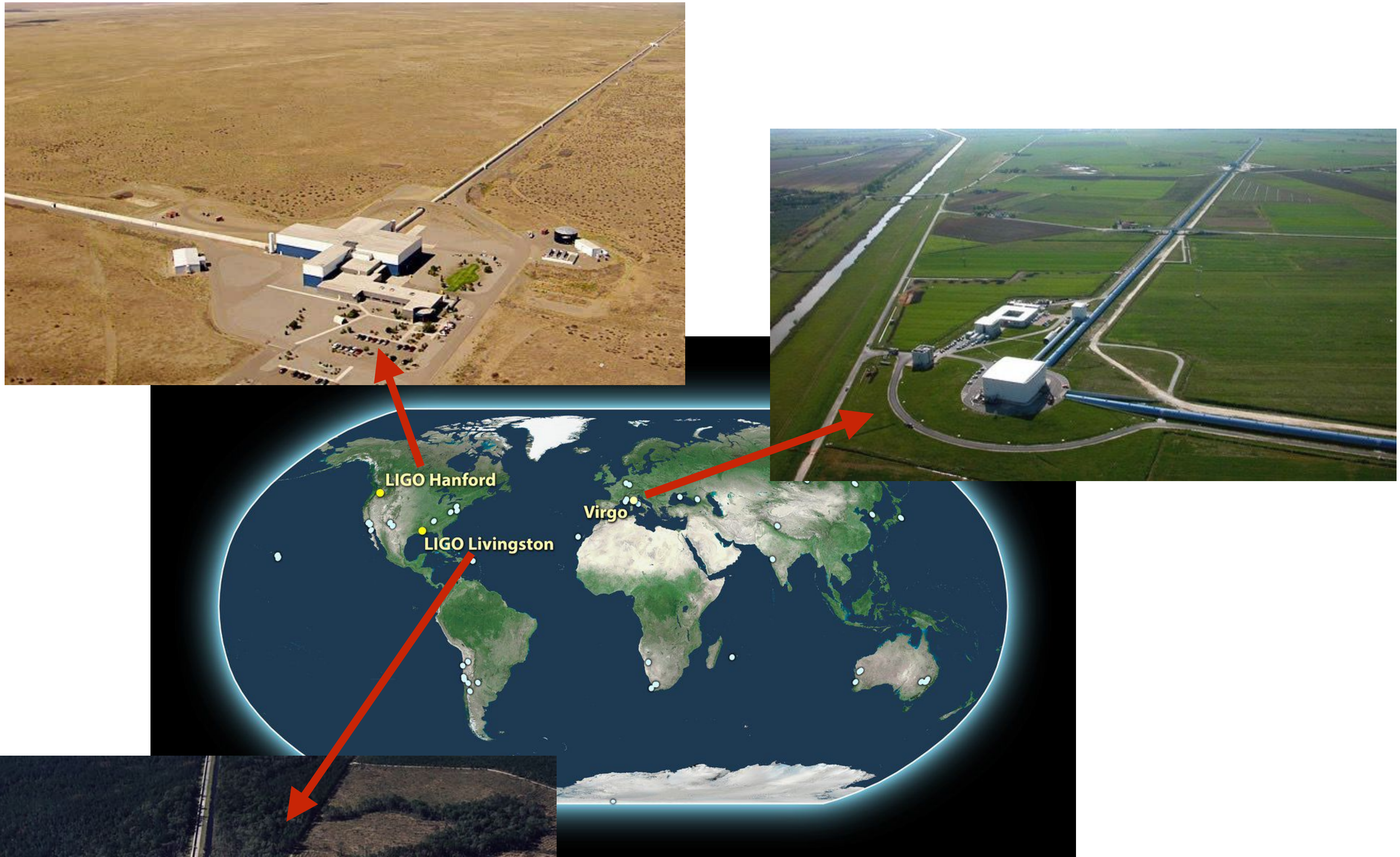

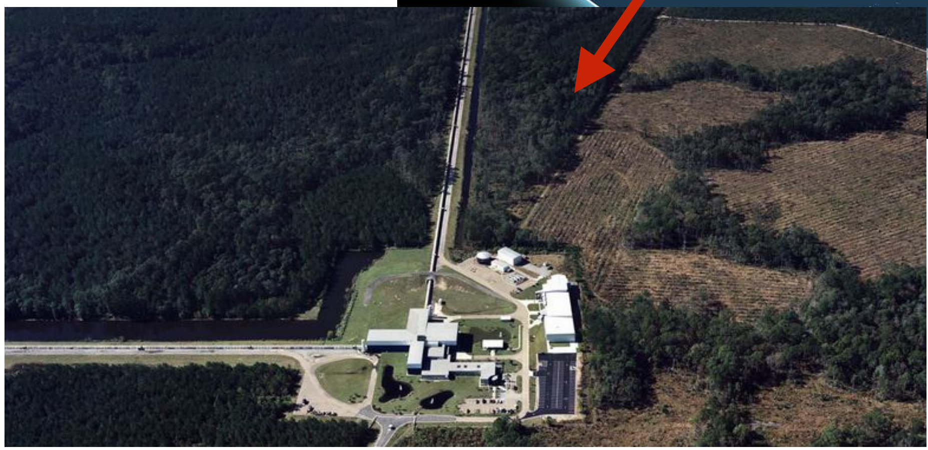

gravitational wave detectors:
LIGO & Virgo

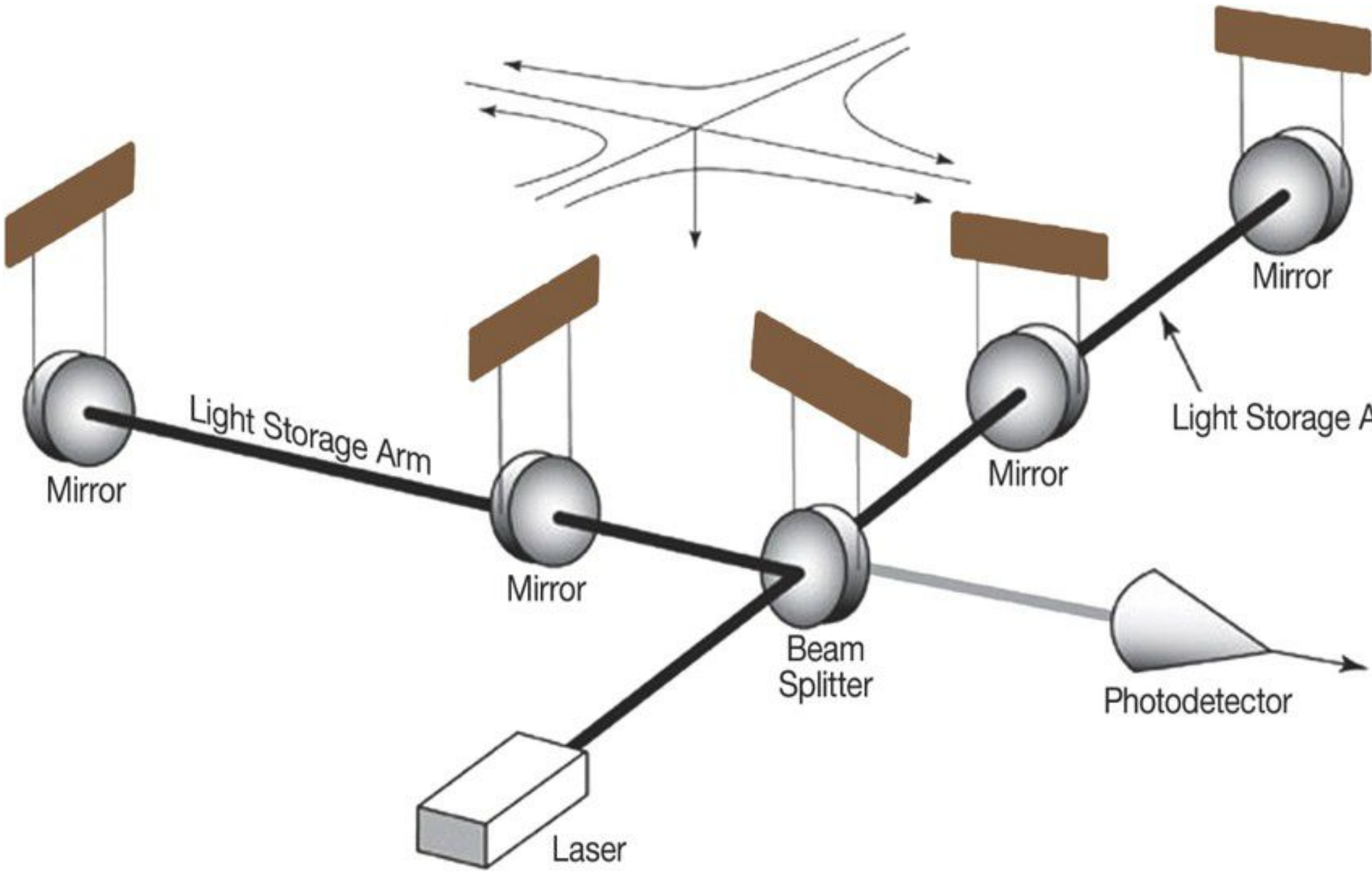

Gravitational waves cause space itself to stretch in one direction and squeeze in a perpendicular direction simultaneously. The effect on LIGO is this: as the wave passes, one arm of an interferometer lengthens while the other shrinks, then vice versa, and so on. The arms will oscillate this way for as long as it takes the wave to pass. As the length of each arm varies, the distance traveled by each laser beam also varies. Consequently, the beam in the shorter arm returns to the beam splitter before the beam in the longer arm. Arriving at different times (one before the other, then after, then before again, etc.) causes the beams to shift in and out of alignment as they merge, experiencing varying levels of destructive and constructive interference as long as the arms change lengths, which is for as long as it takes for the gravitational wave to pass.

First LIGO detection: GW150914

unique characteristics of the signal: direct estimates of the distance, masses, and spins of the merging black holes

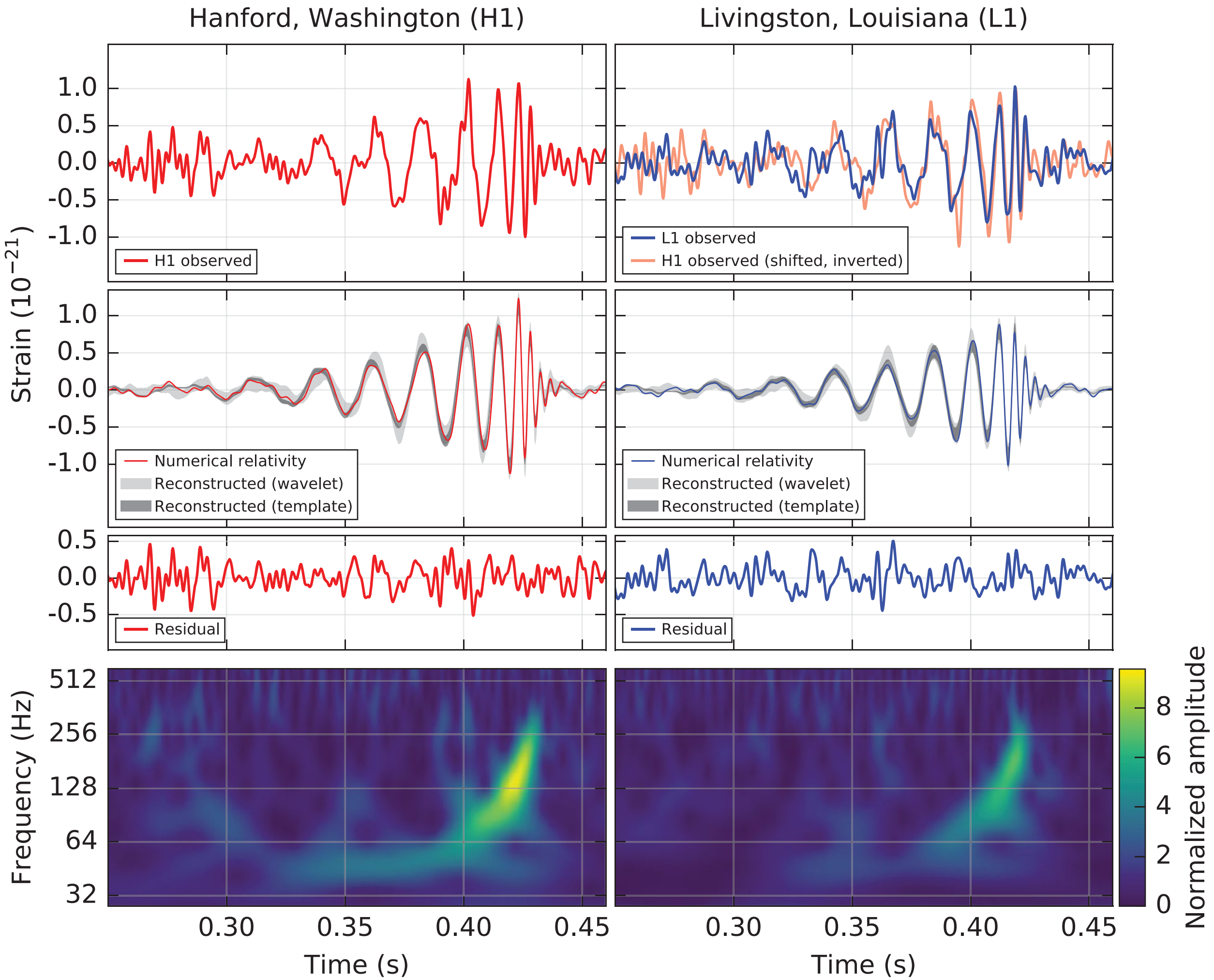

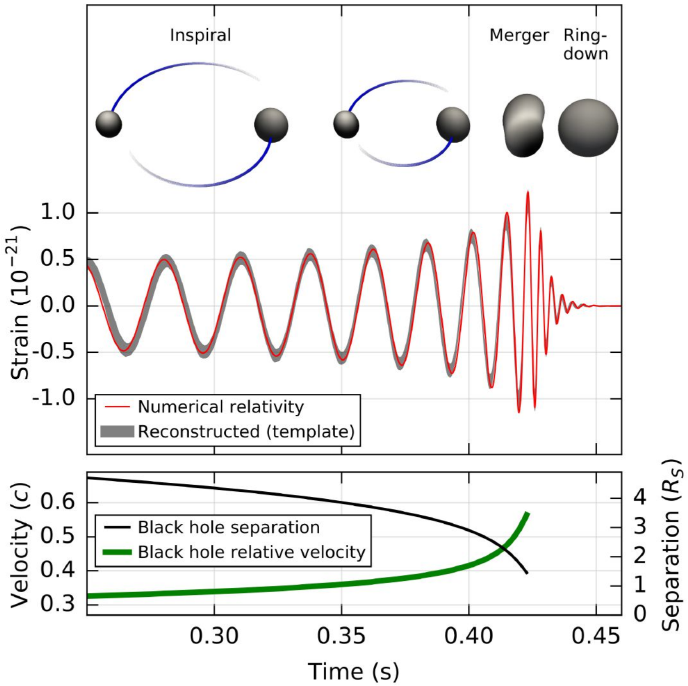

LIGO Collab., 2016

GW150914 — distance 410^{+160}_{-180} Mpc

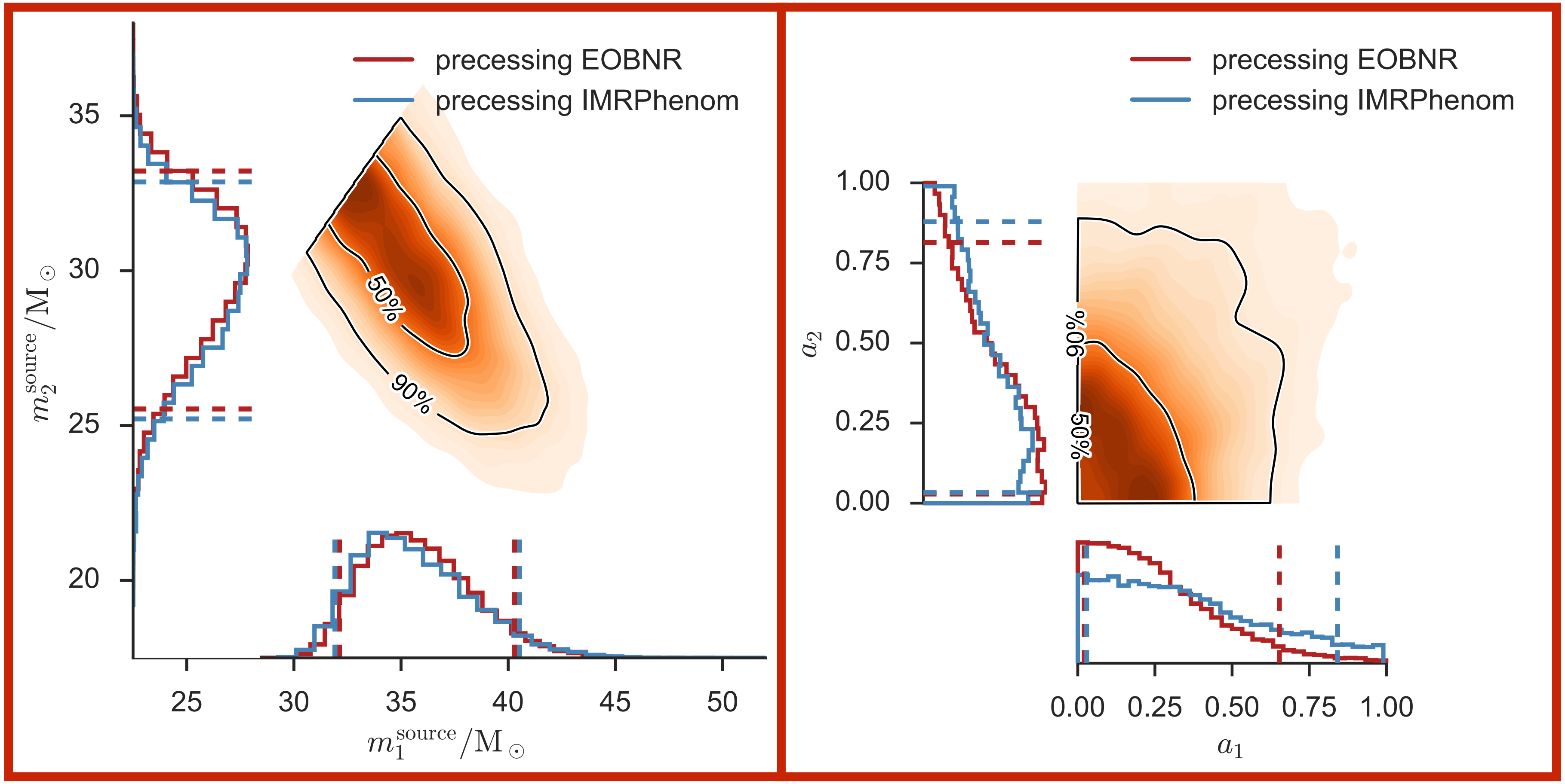

posterior probability densities

LIGO Collab., 2016

Black holes with masses **3-100 M$_\odot$** are formed (*exclusively?*) during the **gravitational collapse** of massive stars at the end of their evolution (-> supernovae!)

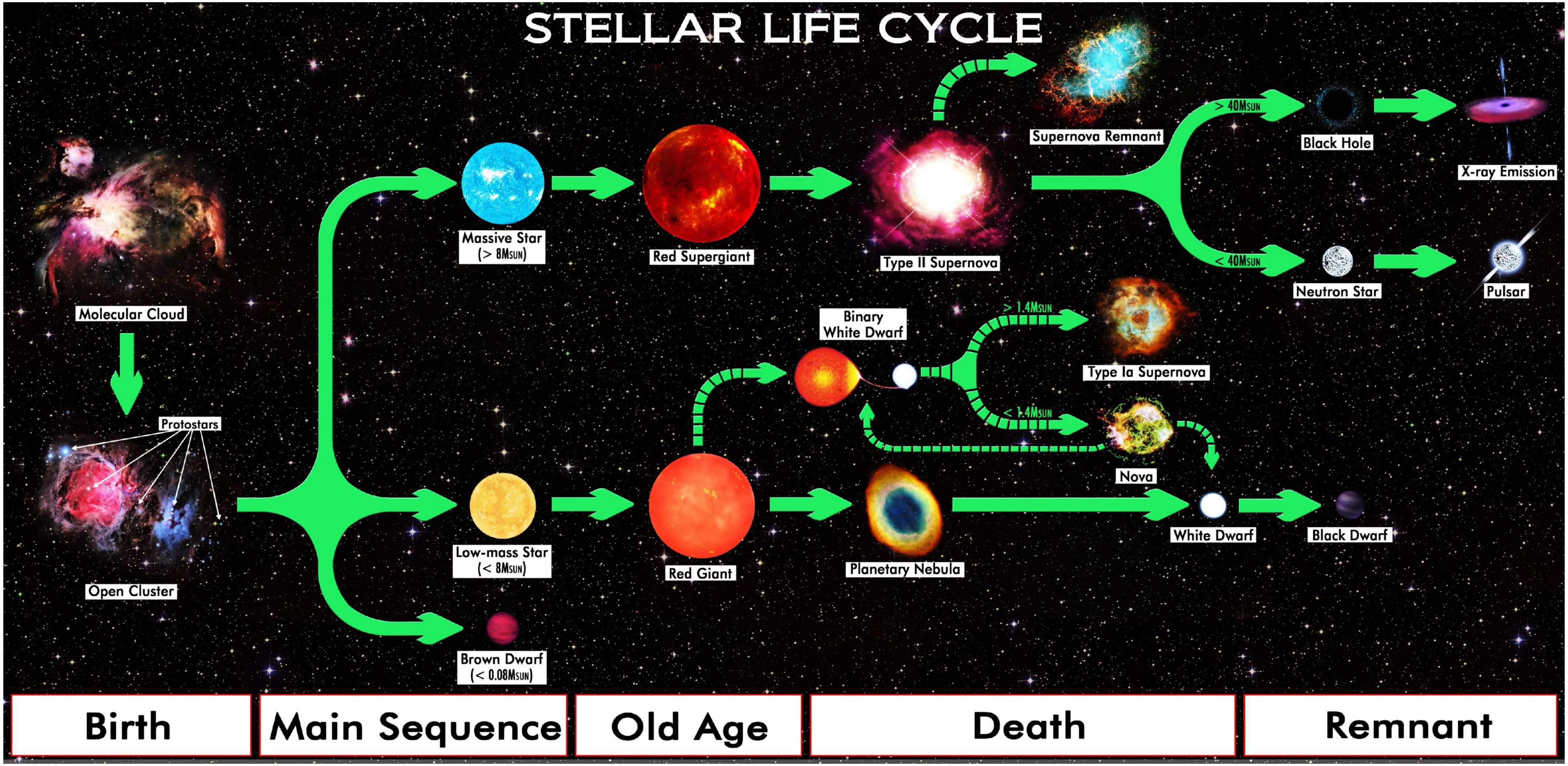

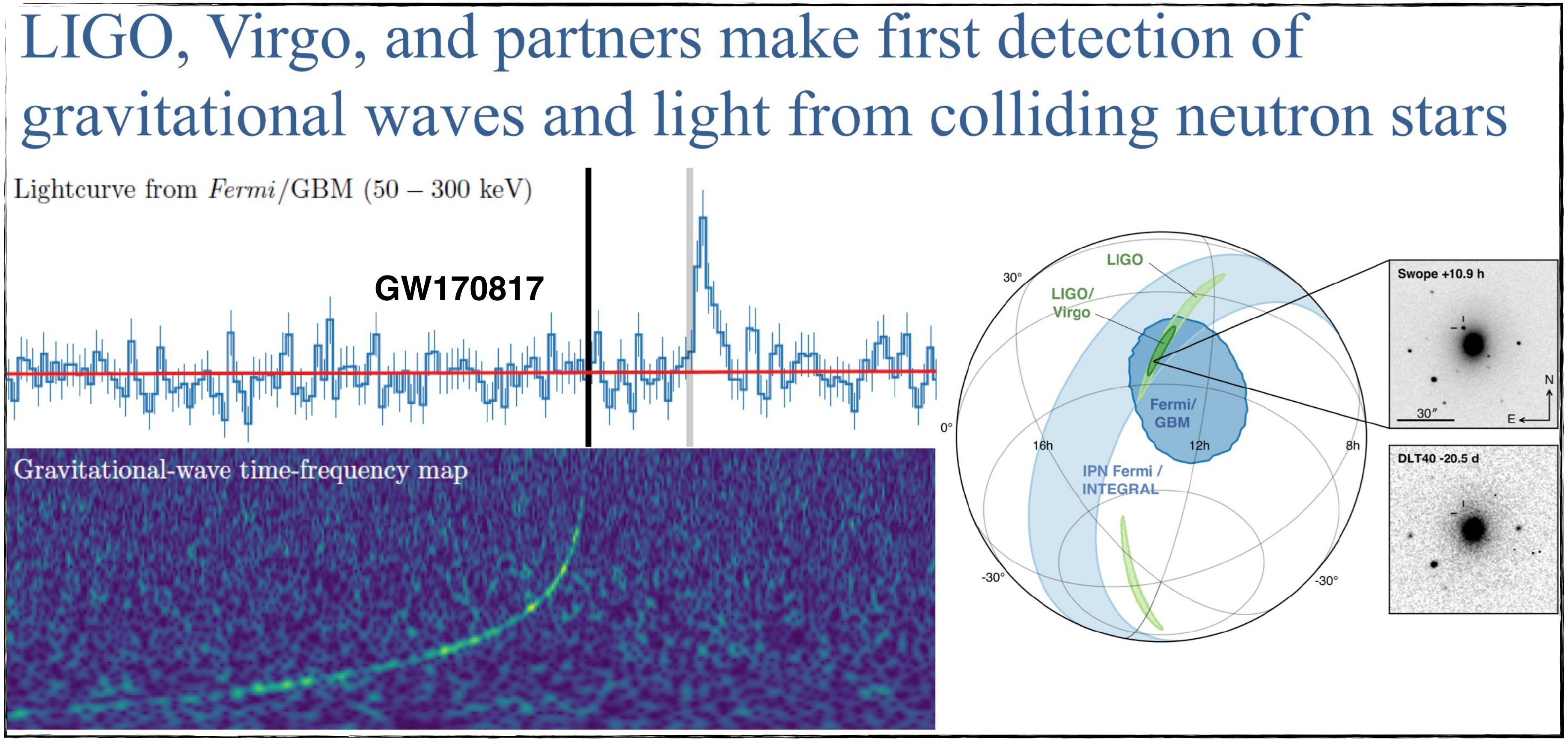

LIGO, VIRGO, Fermi-GBM ++ Collab., 2017

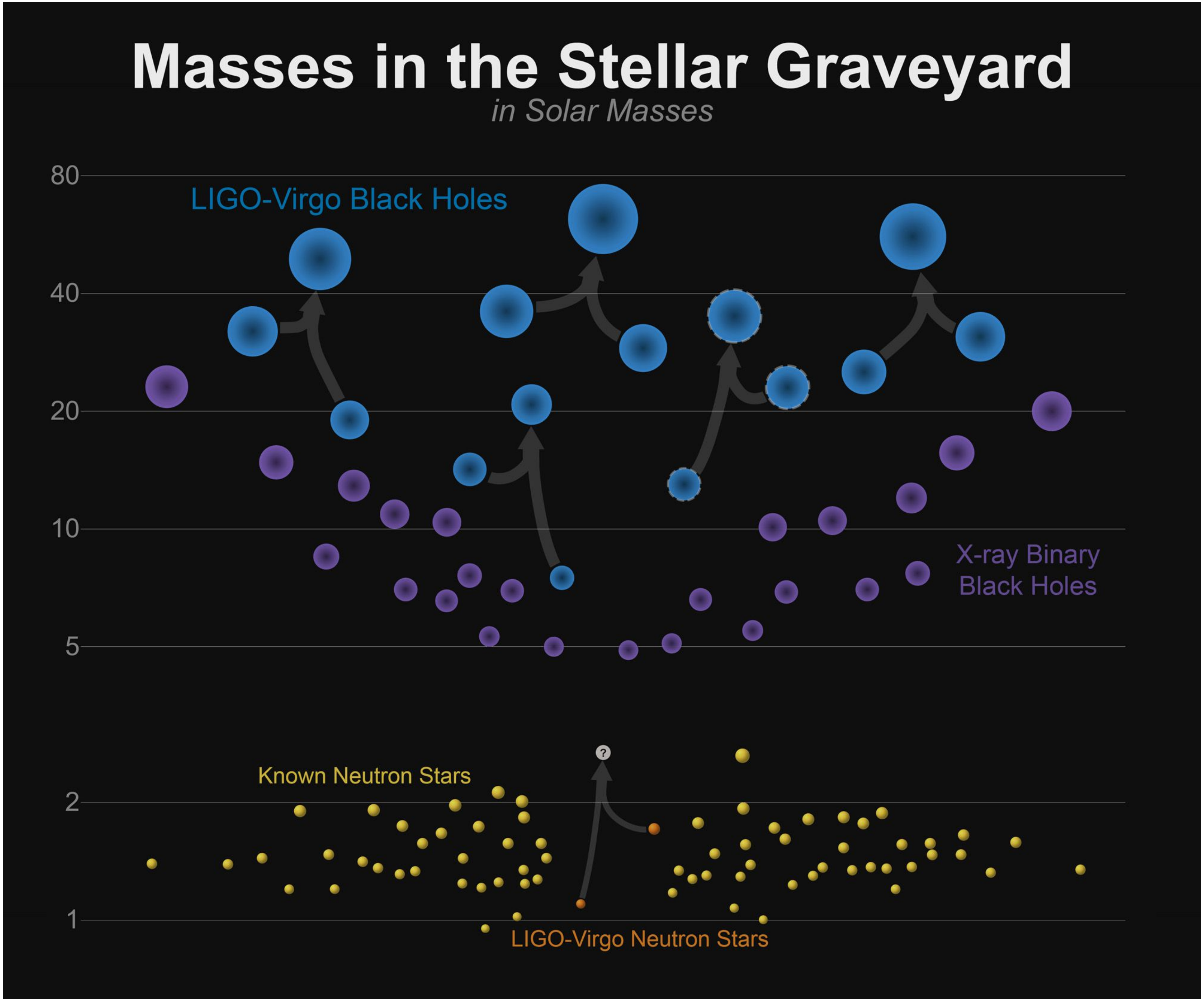

Masses in the Stellar Graveyard
in Solar Masses
80
40
20
10
5
2
1
LIGO-Virgo Black Holes
X-ray Binary
Black Holes
Known Neutron Stars
?
LIGO-Virgo Neutron Stars

JAPAN'S WAVE HUNTER

The Kamioka Gravitational Wave Detector (KAGRA) is the world's fourth major gravitational-wave detector — and Asia's first. Due to open in late 2019, it is the first one to be built underground, and to have cryogenically cooled mirrors, operating at around 20 kelvin. Both innovations should help KAGRA to separate the cosmic ripples from background noise.

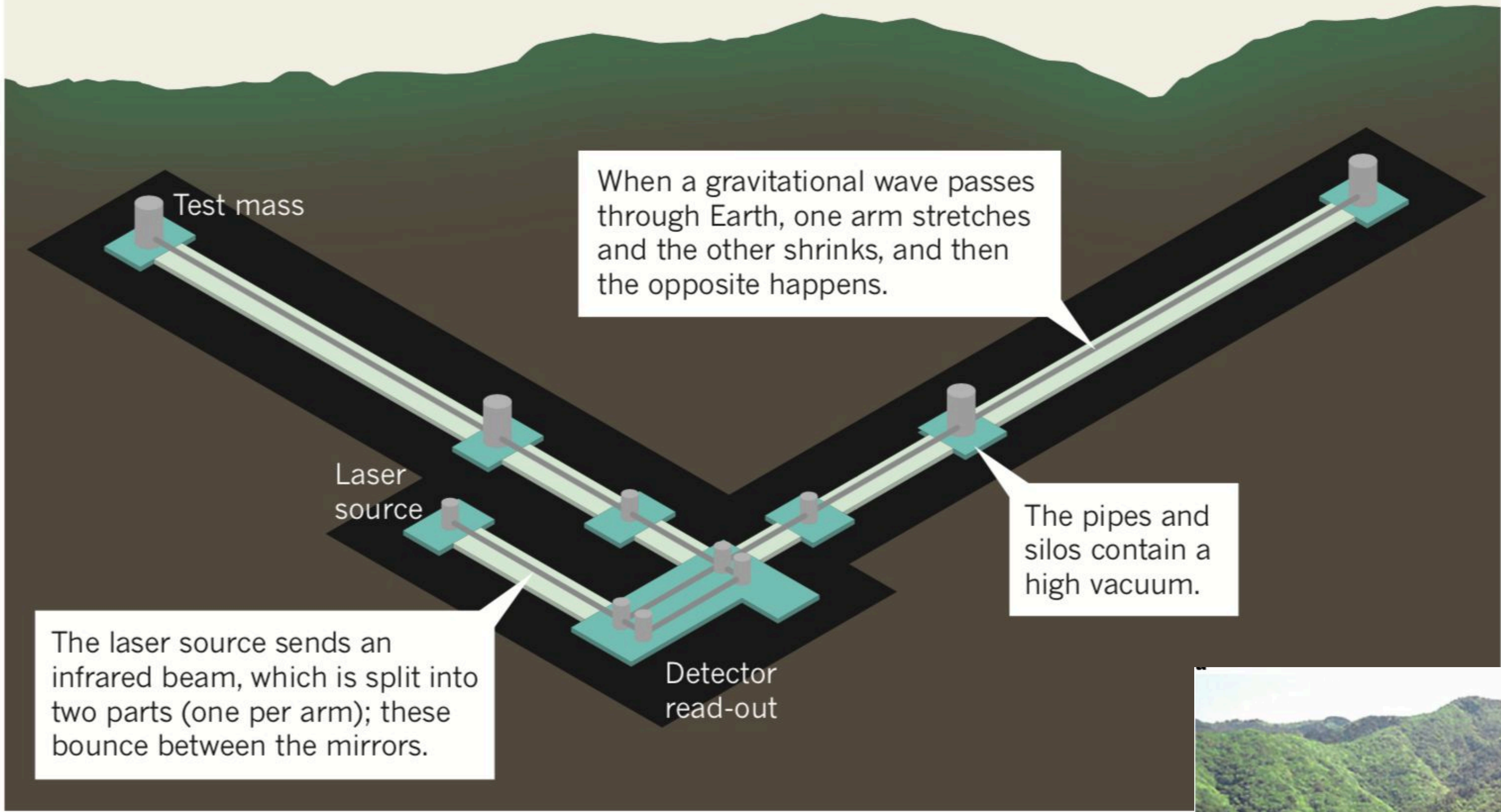

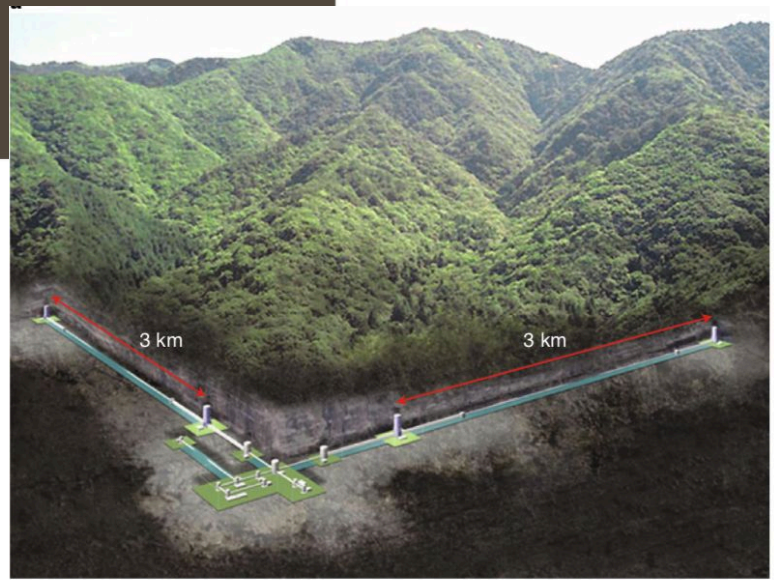

BH X-ray Binaries:

stellar-mass black holes accreting mater from the companion star

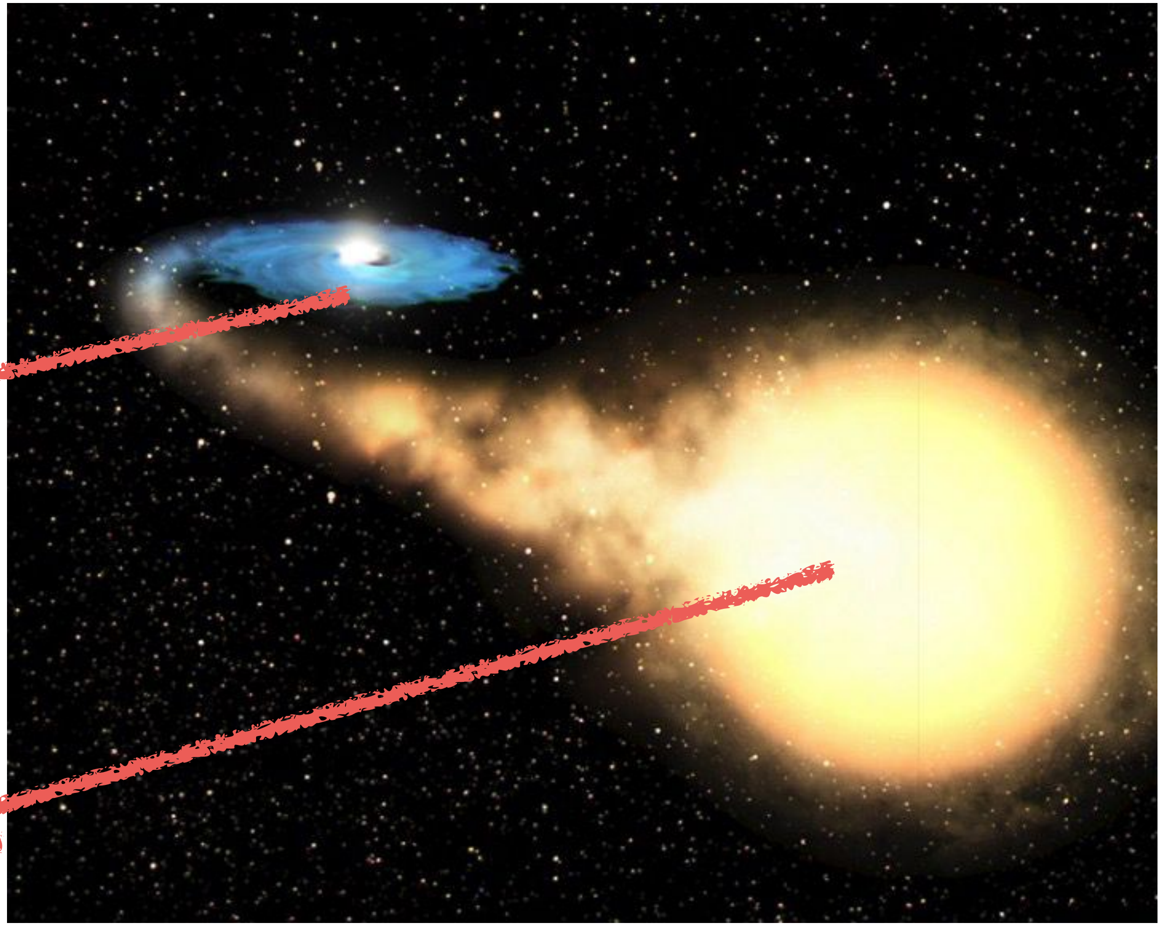

X-ray emission of the accretion disk

optical emission of the companion star

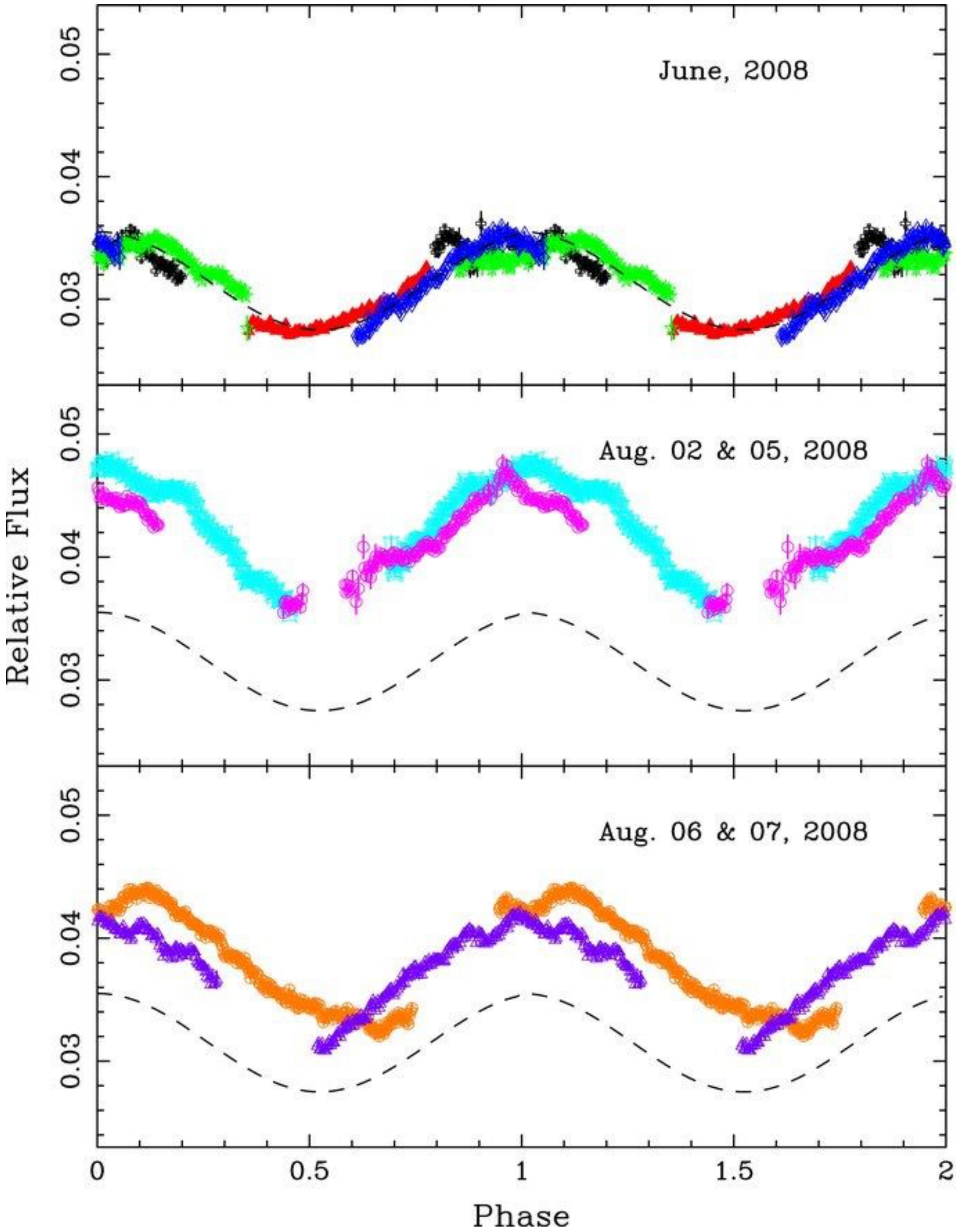

BH mass estimates in X-ray Binaries

orbital modulation of the optical emission (companion star partly eclipsed by the accretion disk)

↓

given the type of the companion (main sequence) star, one may estimate the other dynamical parameters of the system, including the BH mass

V1408 AQUILAE
(Bayless et al. 2011)

No	Name	$M_{comp}[M_\odot]^b$	Spec. type	$M_{BH}[M_\odot]$
1	XTE J1118+480	0.22 ± 0.07	K7/M1V	$6.9 \div 8.2$
2	XTE J1550-564	0.3 ± 0.07	K2/4IV	10.5 ± 1.0
3	GS 2000+25	$0.16 \div 0.47$	K3/6V	~ 6.55
4	GRO J0422+32	~ 0.45	M0/4V	~ 10.4
5	GRS 1009-45	~ 0.5	G5/K0V	~ 8.5
6	GRS 1716-249	~ 1.6	K-M	$\gtrsim 4.9$
7	GX339-4	$0.3 \div 1.1$	KIV	> 7
8	H1705-25	$0.15 \div 1.0$	K3/M0V	$4.9 \div 7.9$
9	A0620-00	0.68 ± 0.18	K2/7V	6.6 ± 0.25
10	XTEJ1650-50(0)	0.7	K4V	~ 5.1
11	XTEJ1859+226	0.7	K5V	7.7 ± 1.3
12	GS2023+338	$0.5 \div 1.0$	K0/3IV	12 ± 2
13	GRS 1124-68	$0.3 \div 2.5$	K5V	6.95 ± 0.6
14	GRS1915+105	0.8 ± 0.5	K1/5III	12.9 ± 2.4
15	GS 1354-64	1.03	G5IV	7.6 ± 0.7
16	GROJ1655-40	1.75 ± 0.25	F3/G0IV	5.31 ± 0.07
17	4U1543-47	$2.3 \div 2.6$	A2V	$2.7 \div 7.5$
18	XTEJ1819-254	$5.49 \div 8.14$	B9III	$8.73 \div 11.70$
19	CygX-1 [b]	19.2 ± 1.9	OI	14.8 ± 0.1
20	LMC X-1[c]	31.79 ± 3.48	O7/O8	10.91 ± 1.55
21	LMC X-3[cf]	3.72 ± 0.24	B5III	7.00 ± 0.32
22	IC 10 X-1[c]	> 17	WNE	> 23.1
23	NGC 300 X-1[c]	26^{+7}_{-5}	WN5	20 ± 4
24	M33 X-7[c]	70.0 ± 6.9	O7/O8 III	15.65 ± 1.45

BH XRBs

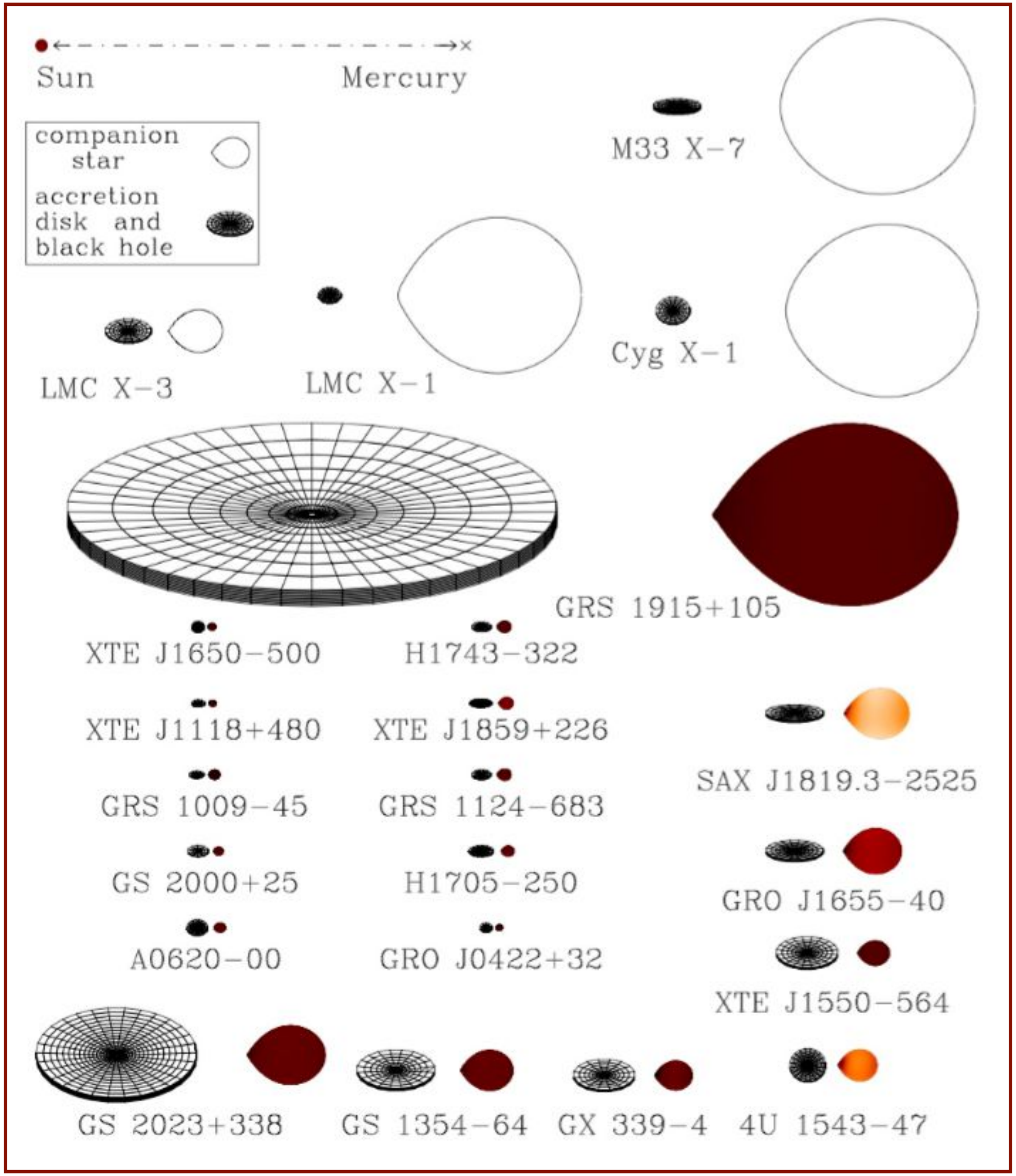

courtesy of J. Orosz

Supermassive BHs

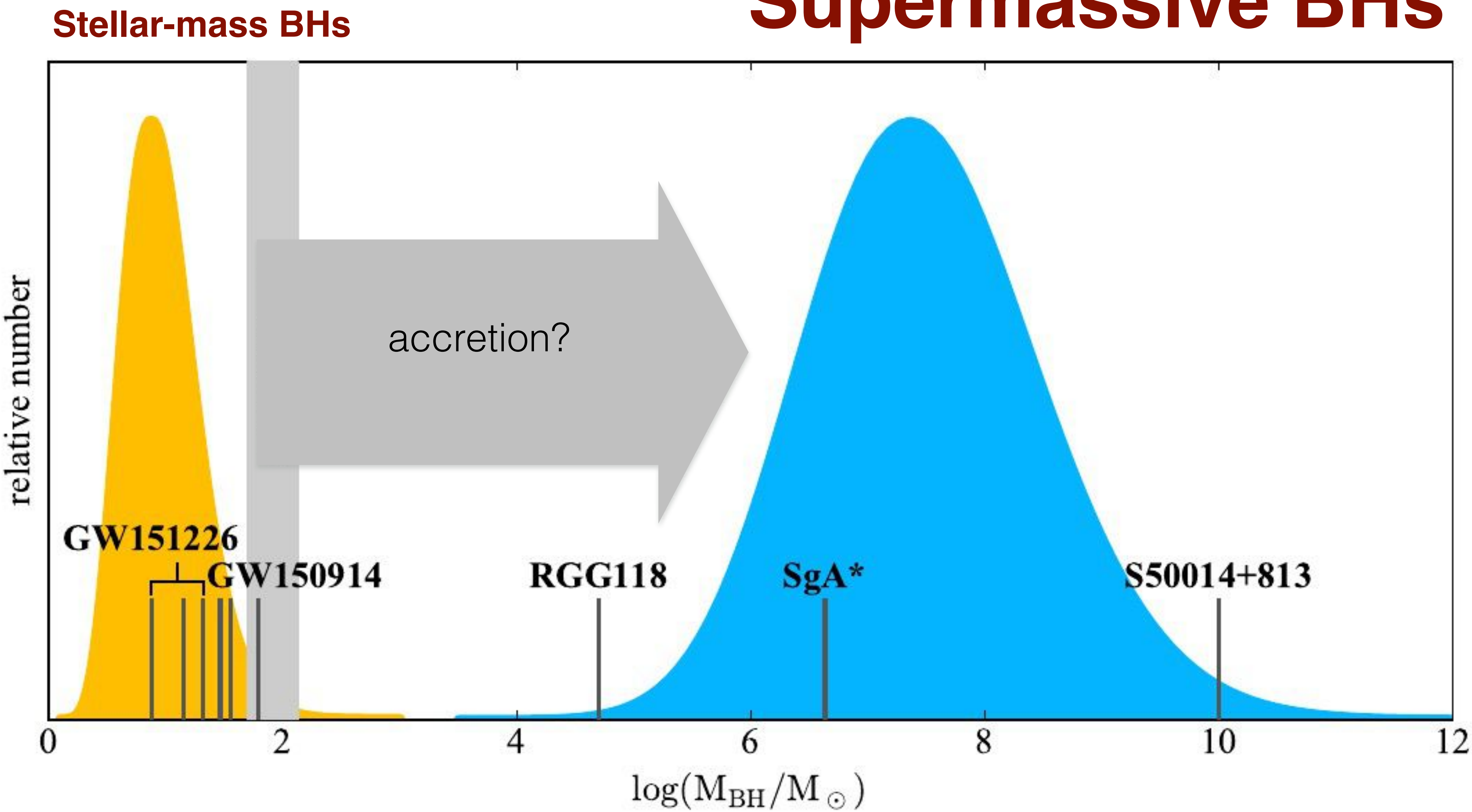

Celoria et al. 2018

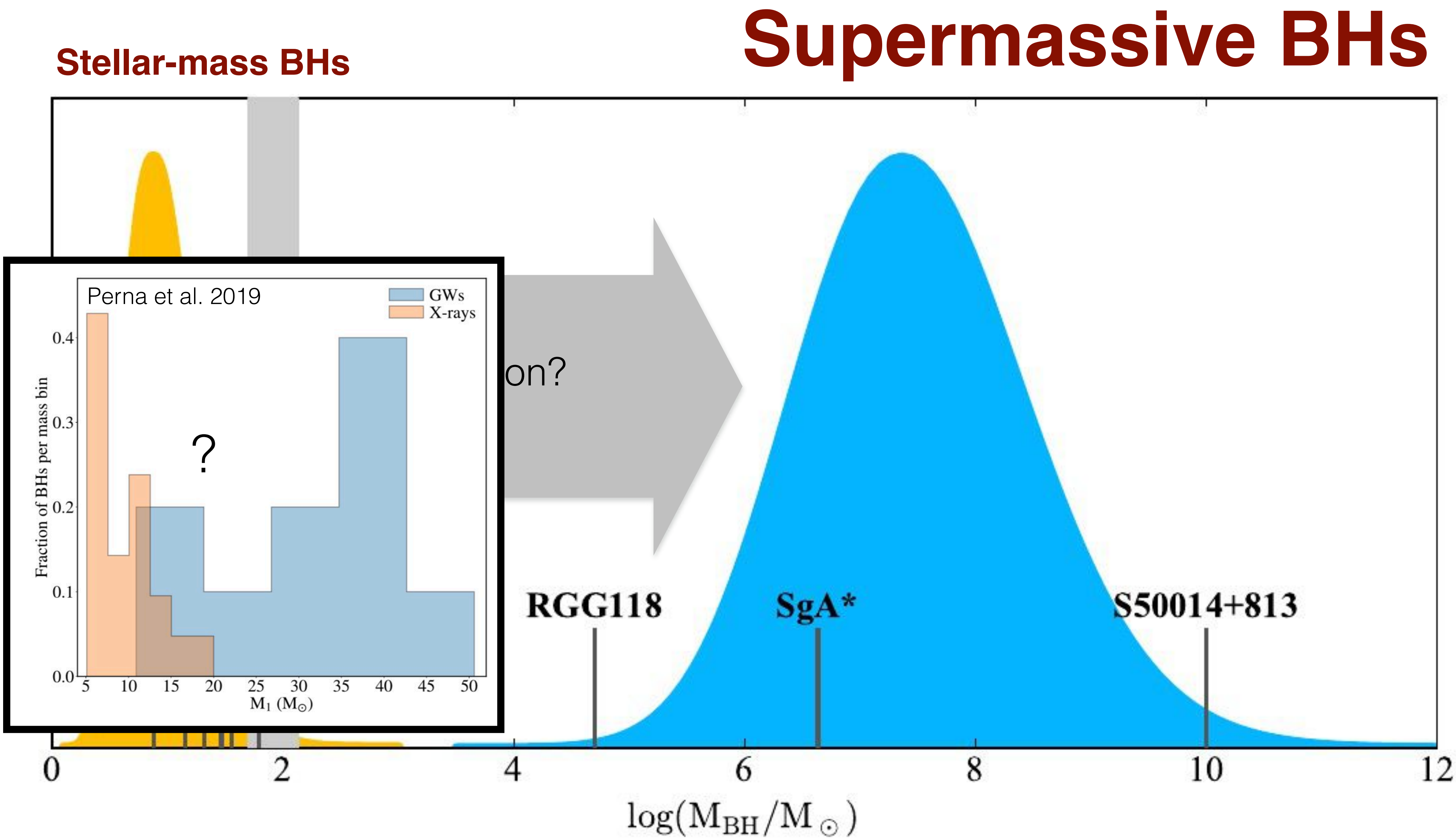
Supermassive BHs
Stellar-mass BHs
Perna et al. 2019
GWs
X-rays
Fraction of BHs per mass bin
?
on?
RGG118
SgA*
S50014+813
M_1 ($M_\odot$)
$\log(M_{BH}/M_\odot)$

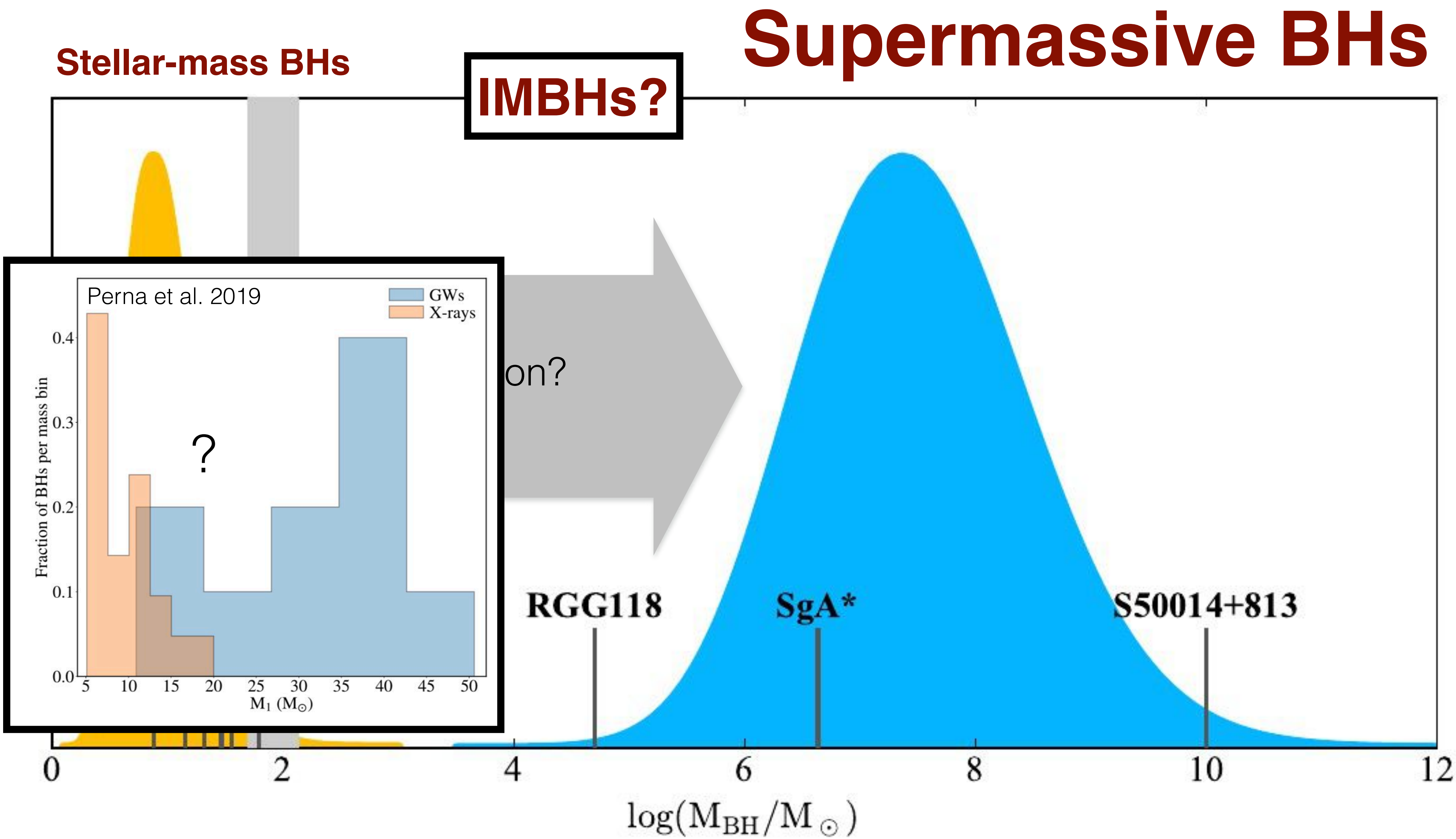

Stellar-mass BHs
IMBHs?
Supermassive BHs
Perna et al. 2019
GWs
X-rays
?
Fraction of BHs per mass bin
M1 (M⊙)
on?
RGG118
SgA*
S50014+813
0
2
4
6
8
10
12
log(MBH/M⊙)

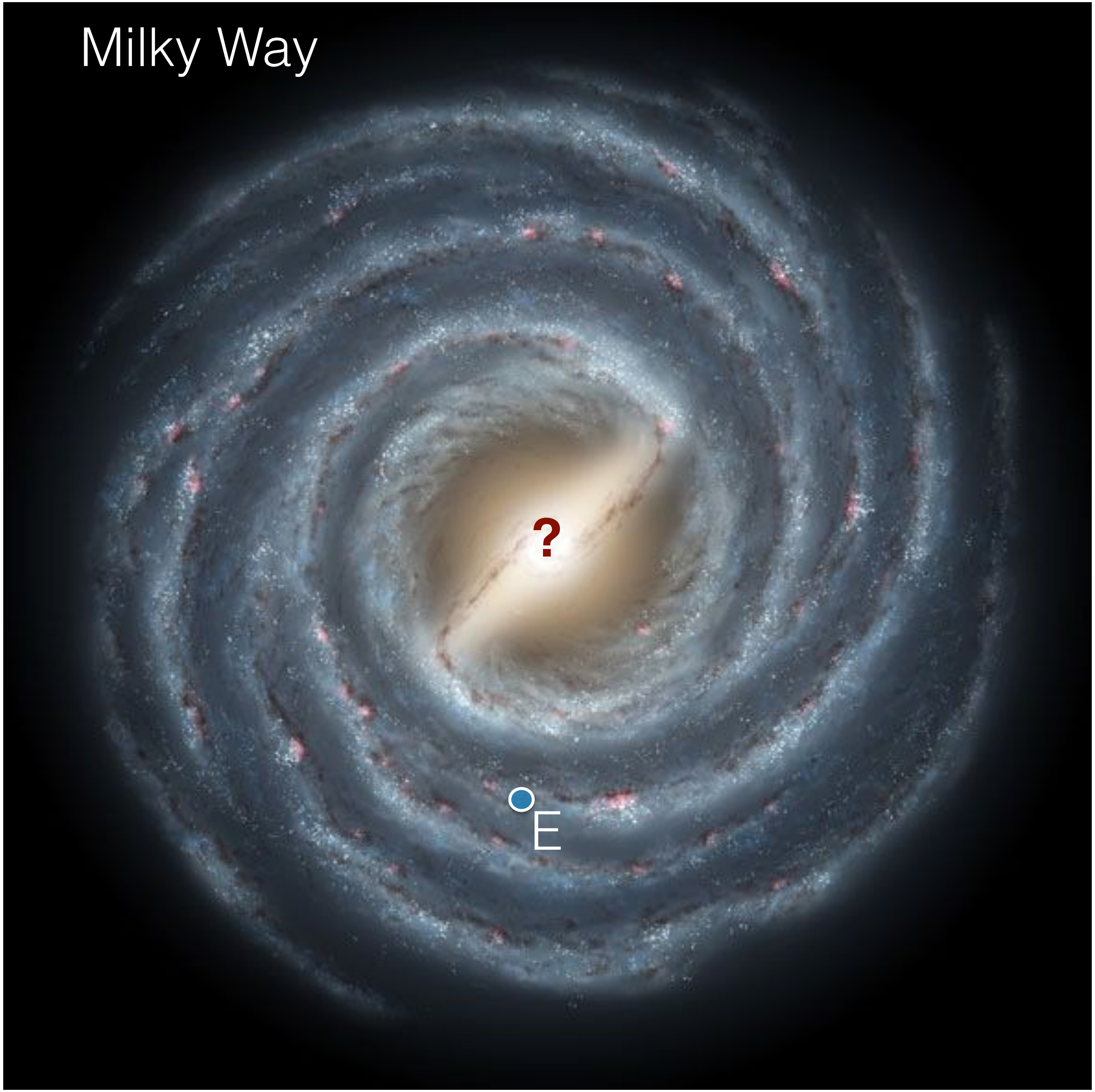

Milky Way
?
E

Galactic Center

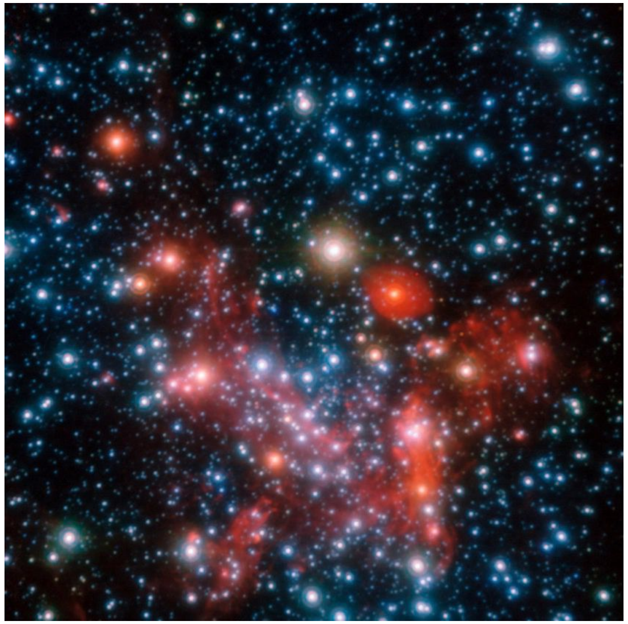

Infrared/optical:
lots of stars and dust

Galactic Center

Infrared/optical:
lots of stars and dust

X-rays:
hot gas and compact sources (XRBs, SNRs, …)

Galactic Center

Infrared/optical:
lots of stars and dust

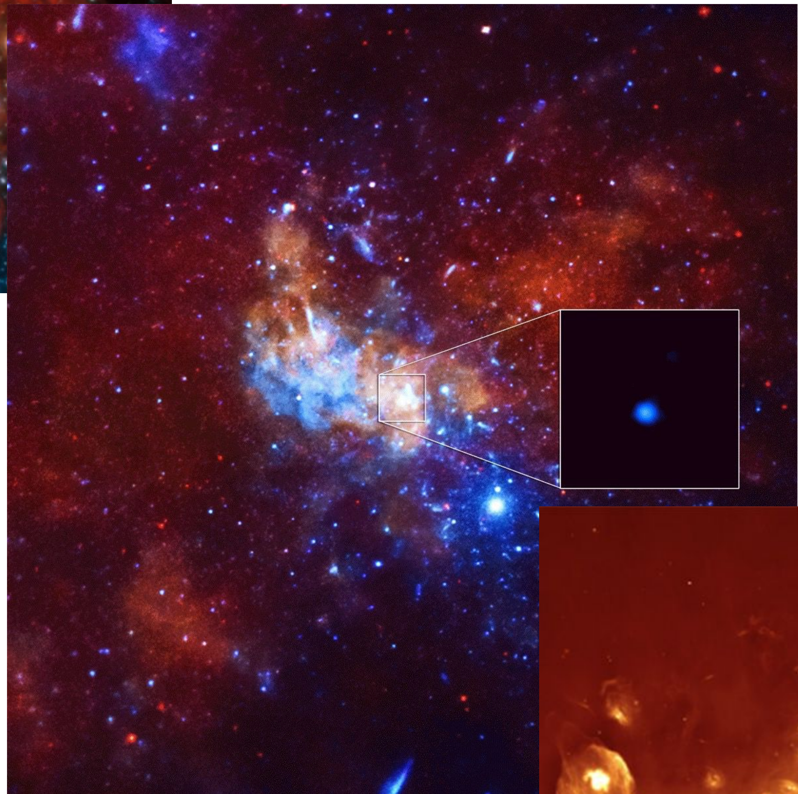

X-rays:
hot gas and compact sources (XRBs, SNRs, …)

Radio:
relativistic magnetised plasma

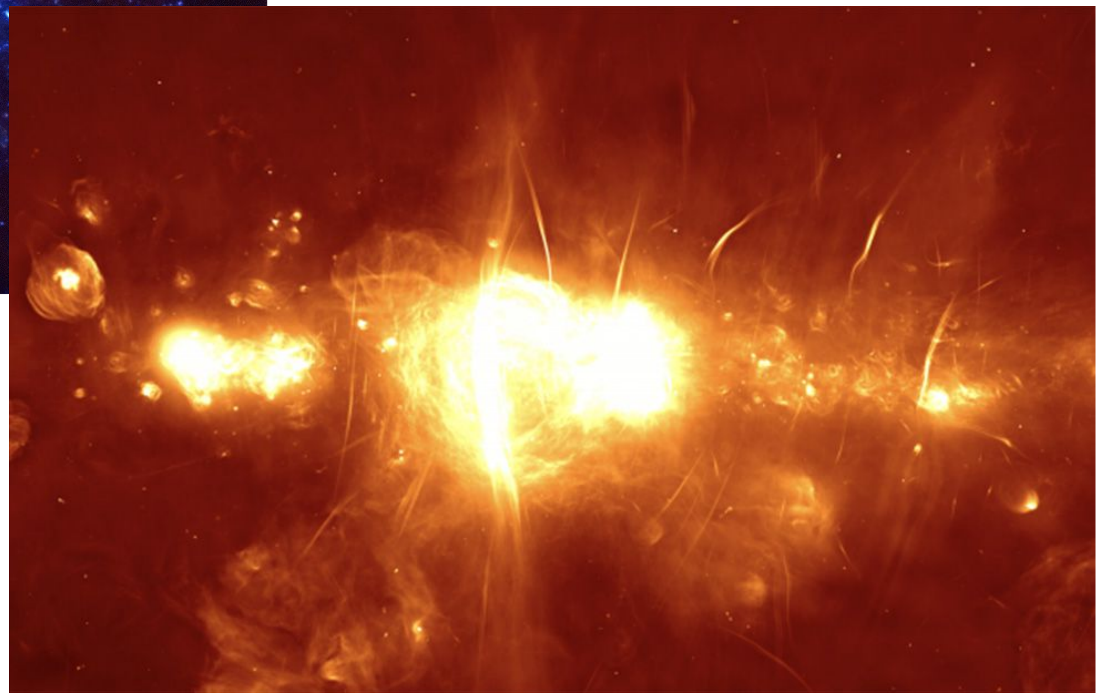

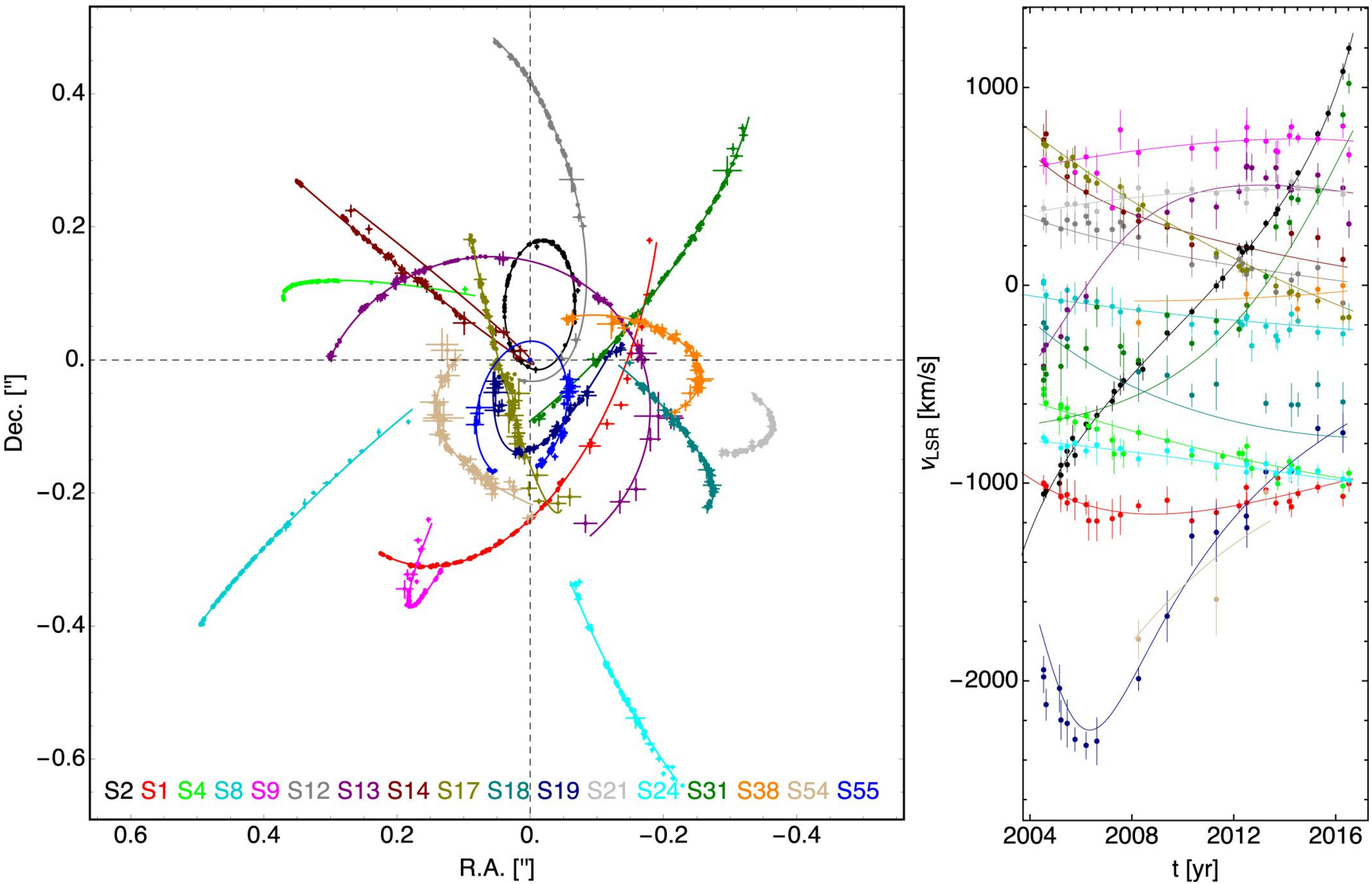

Orbits and radial velocities (along the line of sight) of 17 stars
in the closest neighbourhood of Sgr A*
(Gillessen et al. 2017)

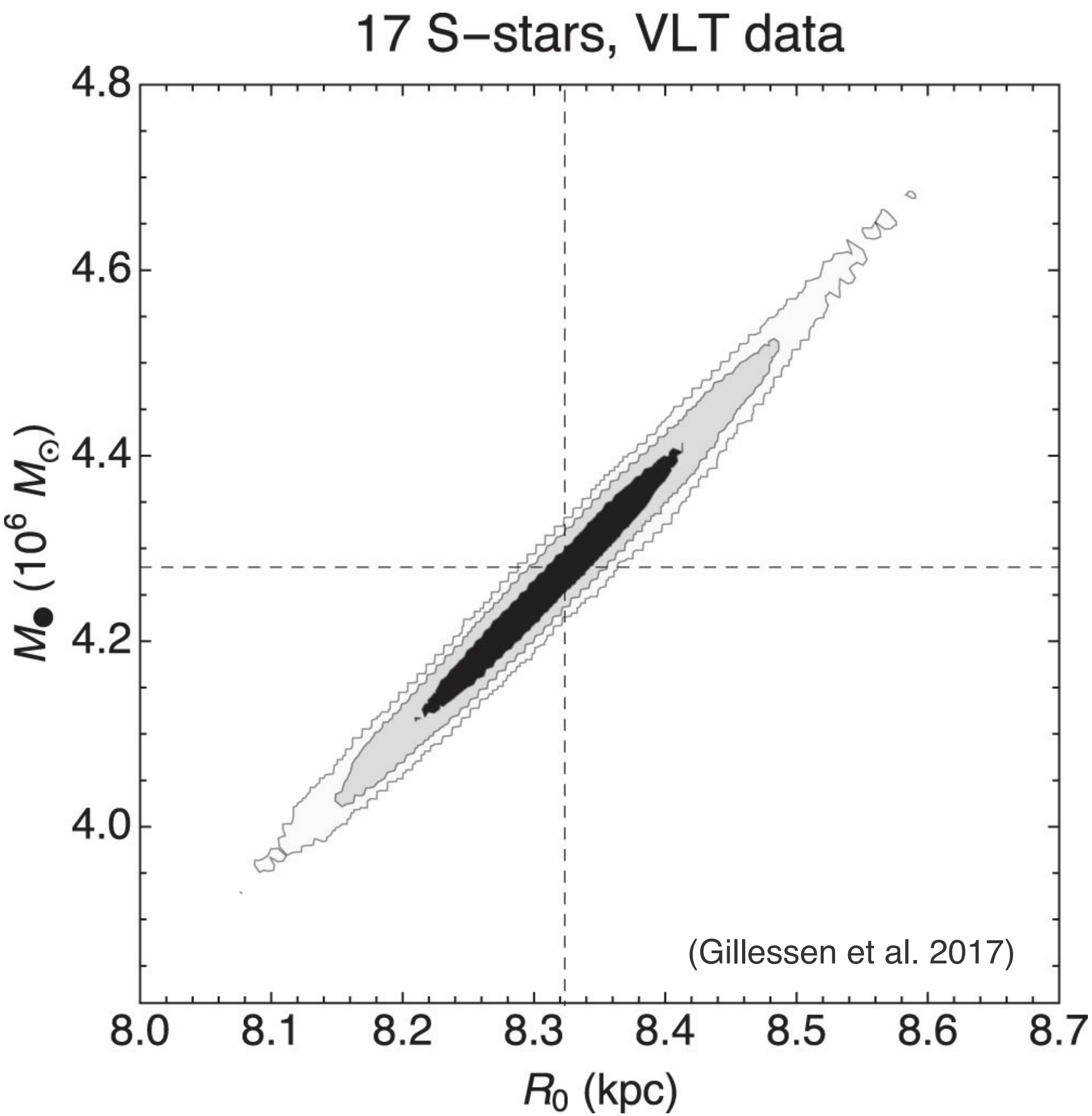

1 kpc $= 3 \times 10^{16}$ km

exact measurements of the mass and the distance of the SMBH residing in the center of our Galaxy!

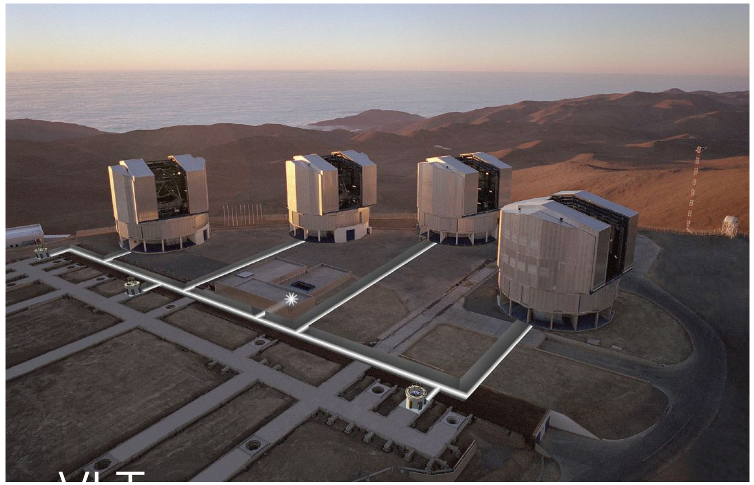

Can we resolve the Sgr A* horizon?

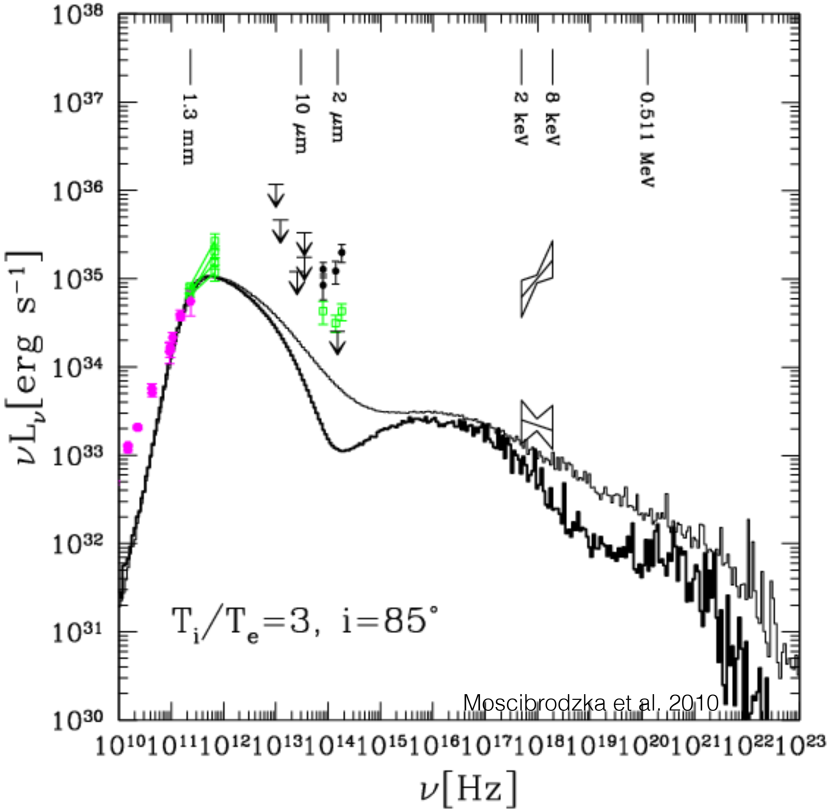

due to very low accretion rate of Sgr A*, its accretion disk should be pronounced not only in X-rays, but also at radio frequencies ("Radiatively Inefficient Accretion Flow", with de-coupled electron and proton temperatures, and hence broad-band emission continuum)

->

good news, as radio interferometers are of a much better angular resolution than the currently operating X-ray telescopes (in particular *Chandra*, with ~arcsec resolution)

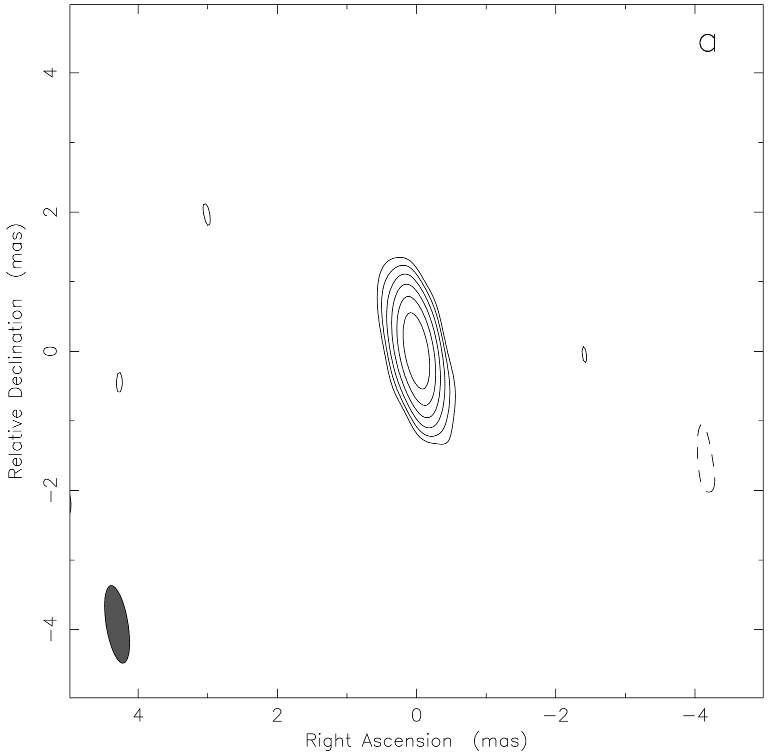

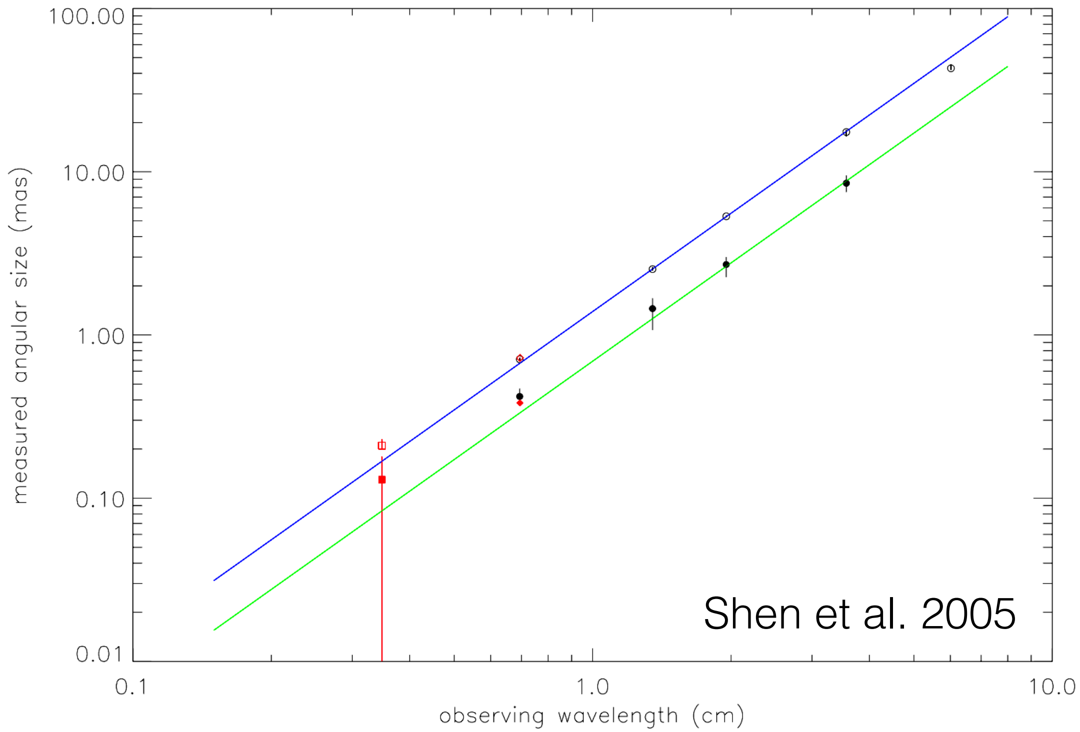

VLBA observations with very high angular resolution (~0.2mas) at 3.5mm:
upper limit for the radio size of Sgr A*
0.1 mas -> ~10^8 km ~1 AU

event horizon of Sgr A*
(assuming zero angular momentum)
r_S ~ 10^7 km ~ 0.1 AU -> 0.01 mas

The **Event Horizon Telescope** (**EHT**)
is a project to create a large telescope array consisting of a global network of radio telescopes and combining data from several very-long-baseline interferometry (VLBI) stations around the Earth

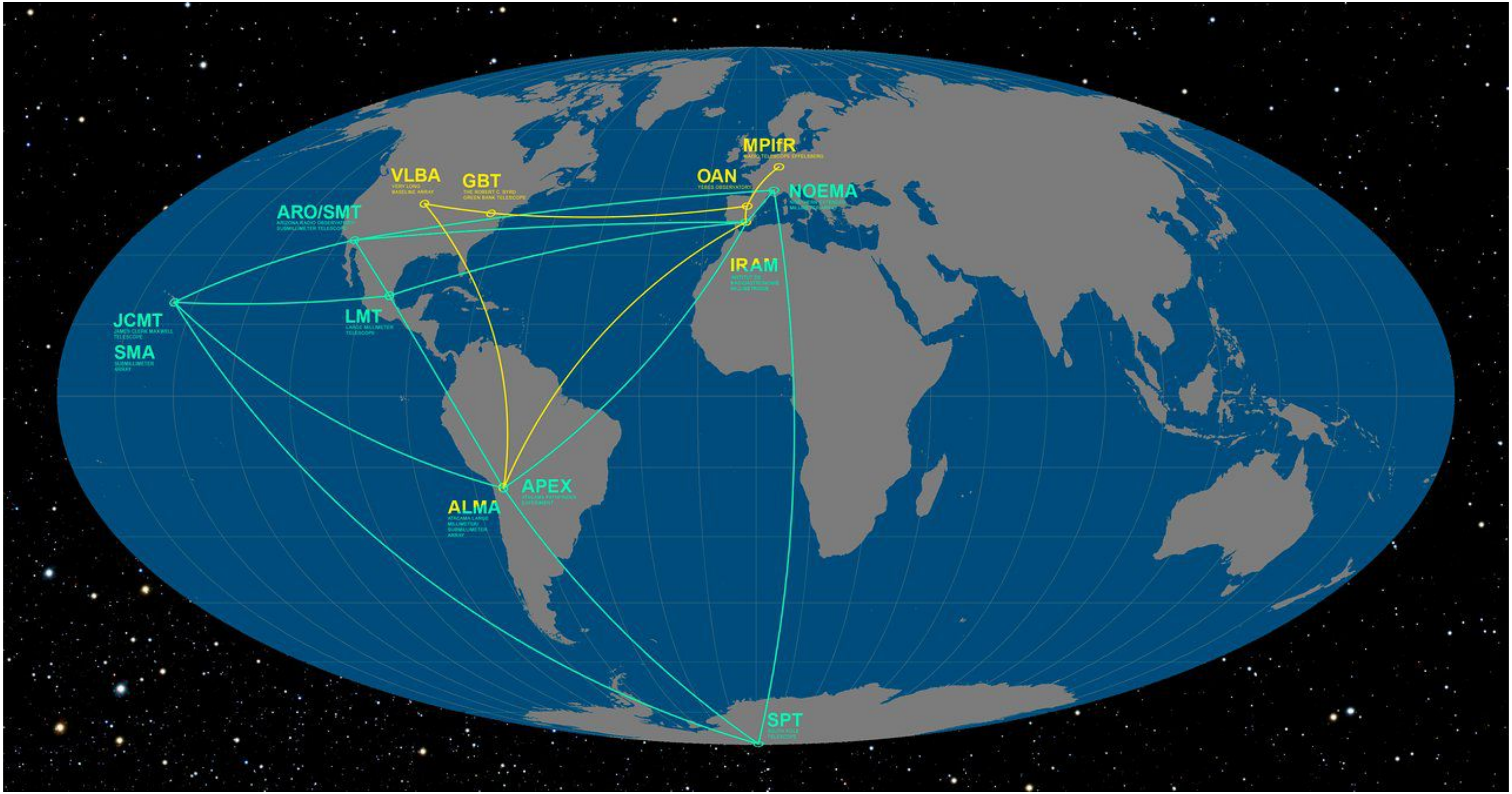

Imaging of the Sgr A* event horizon with the EHT

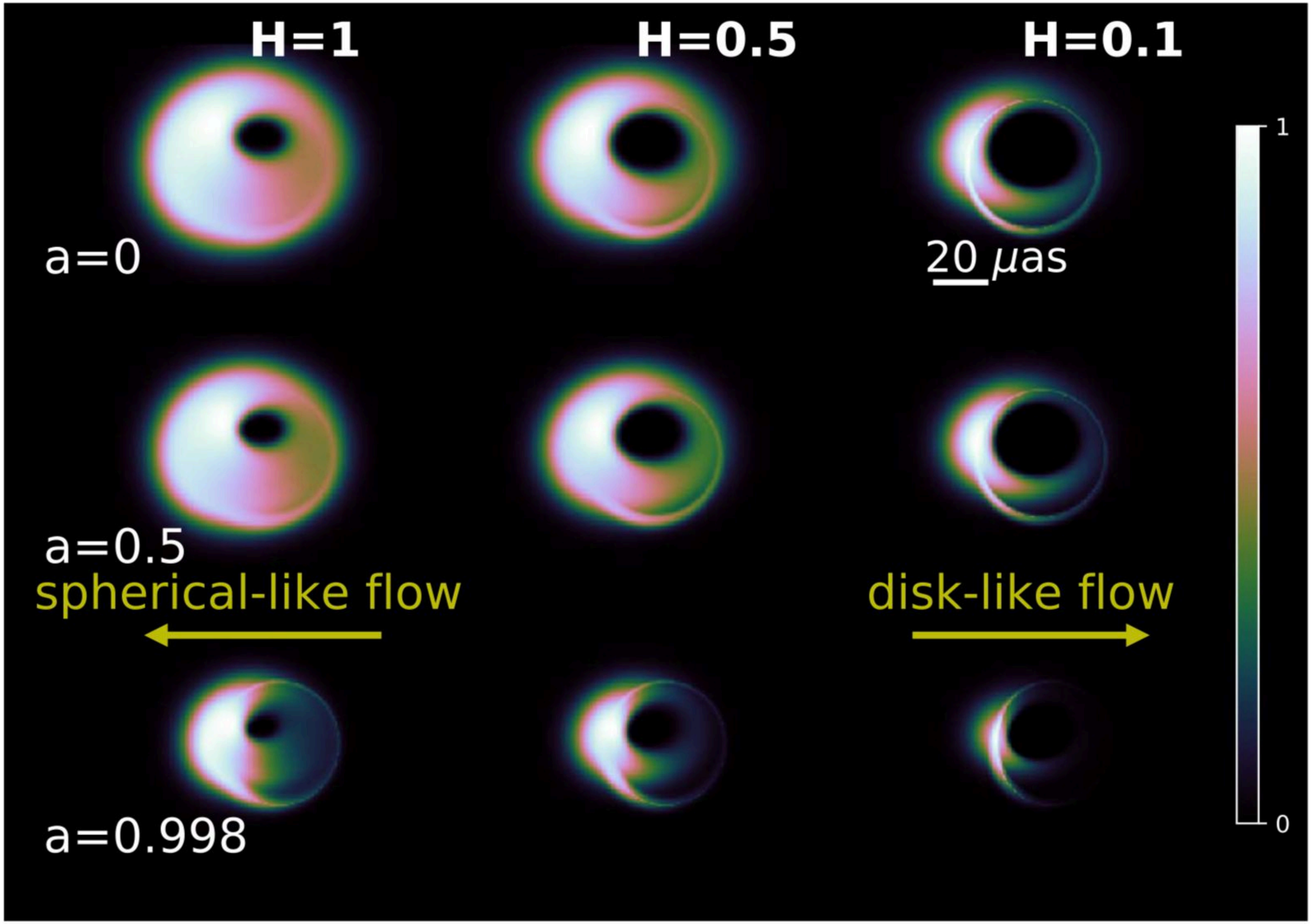

Pu & Broderick 2018

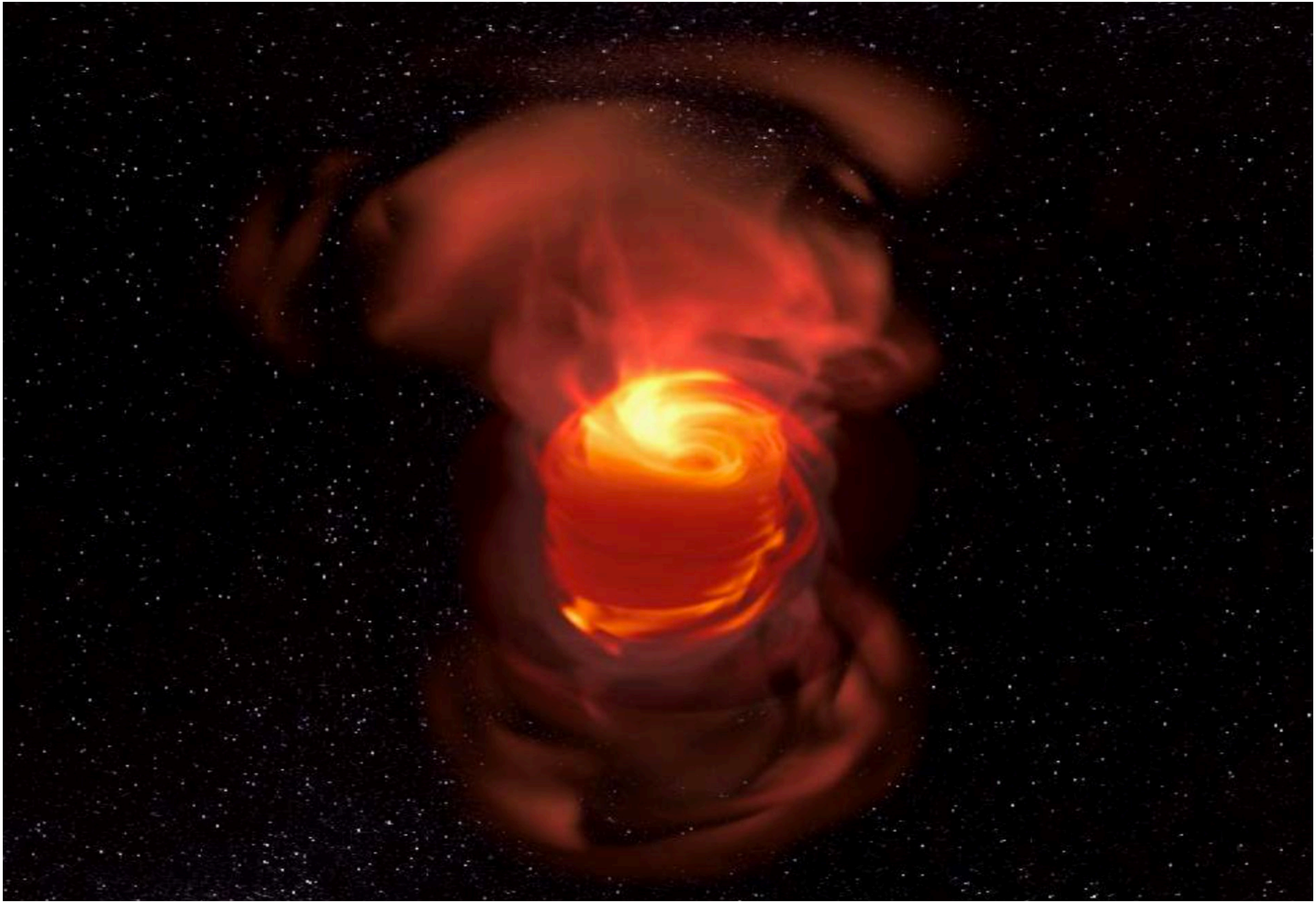

Virgo A (M87)

- low-power but nearby radio galaxy, hosted by the dominant galaxy in the Virgo cluster
- complex radio outflow interacting with the intracluster medium

Virgo A (M87), distance 16 Mpc

- radio outflow can be traced from kpc scale down to sub-pc scale

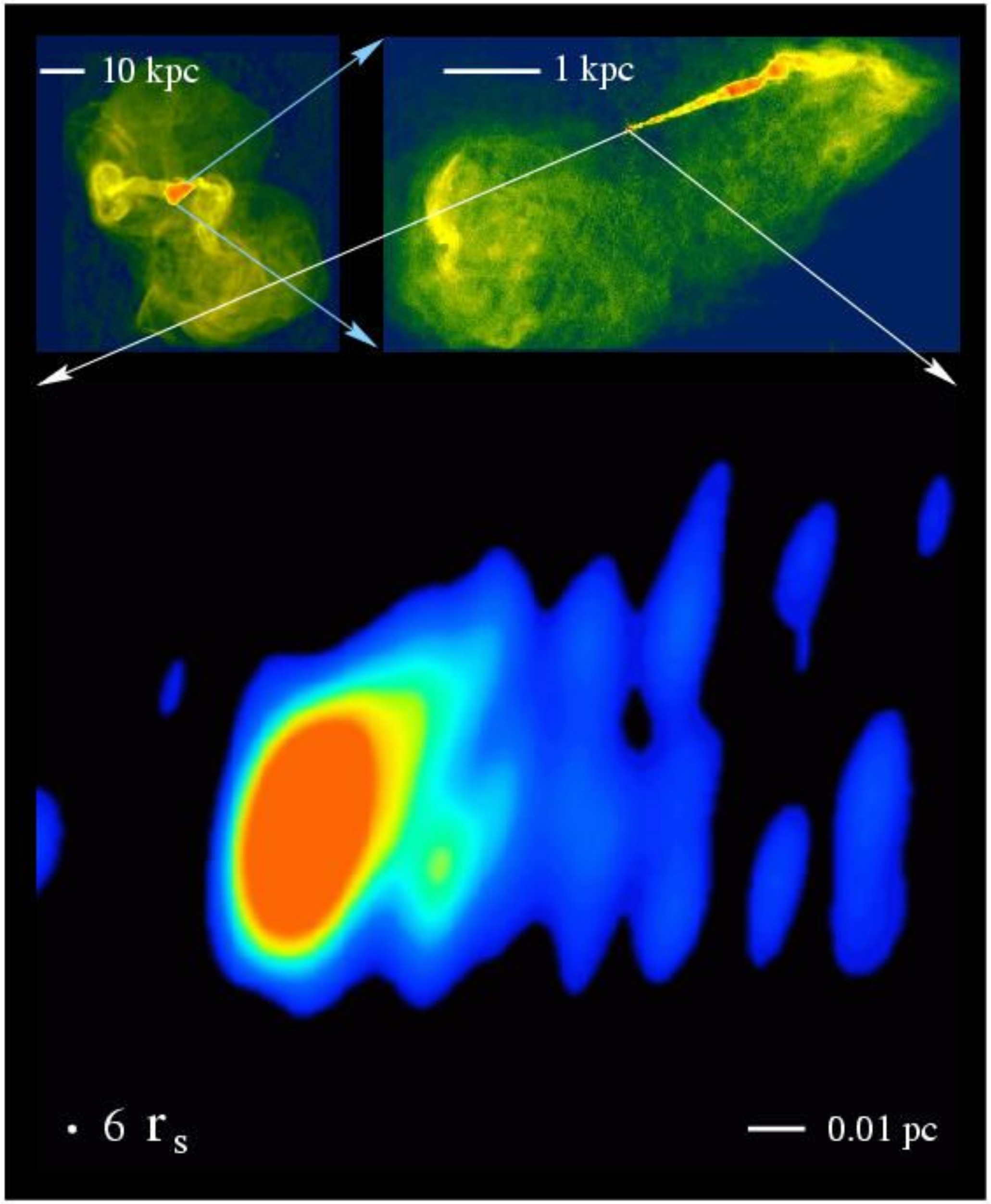

The EHT 2017 campaign

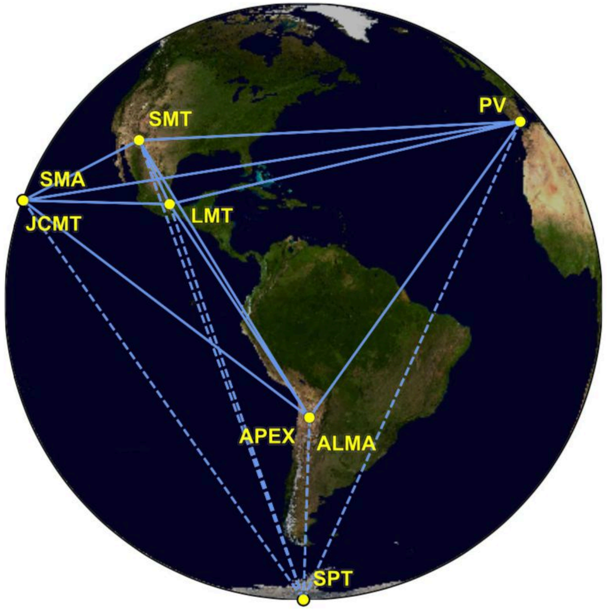

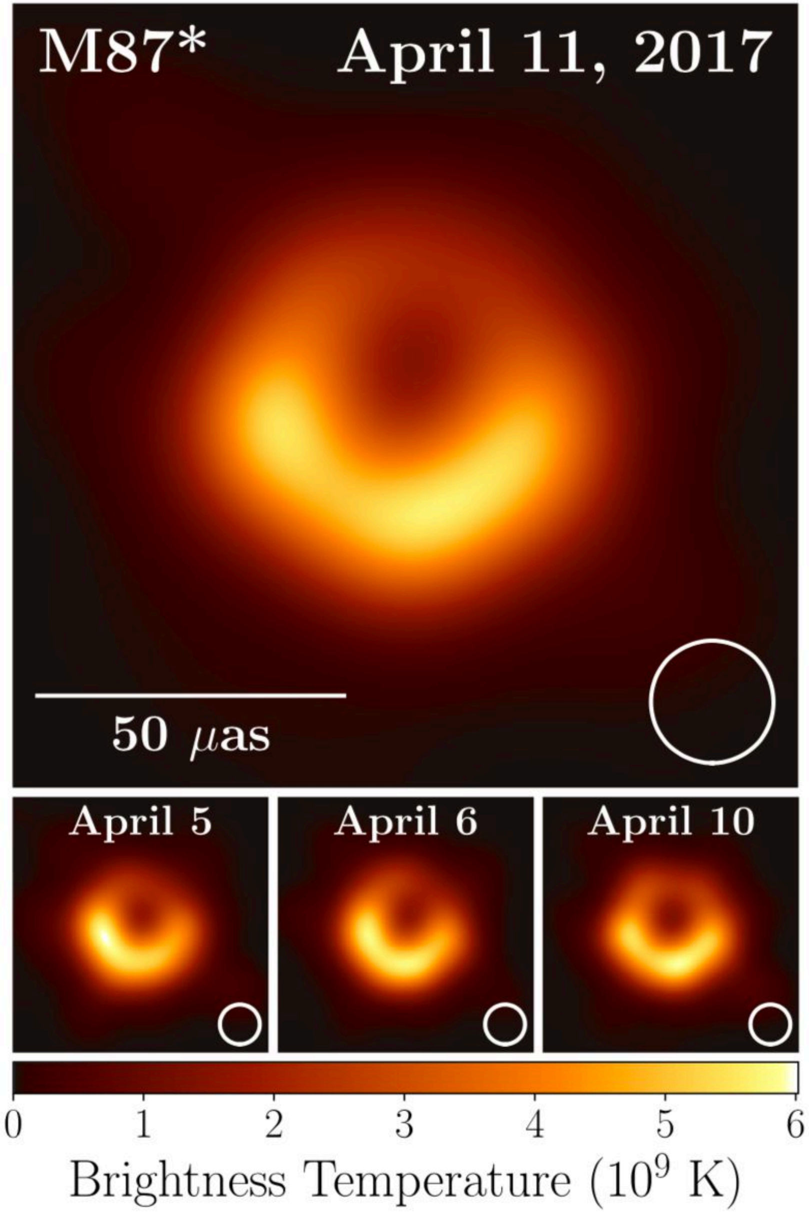

<u>The EHT Collab. 2019:</u>

“Comparing the data with an extensive library of synthetic images obtained from GRMHD simulations covering different physical scenarios and plasma conditions (…) allows us to derive an estimate for the black hole mass of

$M_\bullet = (6.5 \pm 0.7) \times 10^9\ M_\odot$

Based on our modeling and information on the inclination angle, we derive the sense of rotation of the black hole to be in the clockwise direction, i.e., the spin of the black hole points away from us. The brightness excess in the south part of the emission ring is explained as relativistic beaming of material rotating in the clockwise direction as seen by the observer, i.e., the bottom part of the emission region is moving toward the observer.”

SMBH sphere of influence

event horizon (for *a=0*)

$$r_S = \frac{2G\mathcal{M}_\bullet}{c^2} \quad \approx 10^{-8} \left(\frac{\mathcal{M}_\bullet}{10^8 M_\odot}\right) \text{kpc}$$

radius of the "sphere of influence" of the SMBH, i.e. the distance at which its gravitational potential significantly affects the motion of the stars or of the interstellar medium (for the velocity dispersion **σ** of the stars within the inner parts of the galaxy, i.e. spheroidal component whose stellar dynamics is dominated by random motions, not by rotation)

$$\frac{1}{2}\sigma^2 = \frac{G\mathcal{M}_\bullet}{r_i} \quad \longrightarrow \quad r_i = \frac{2G\mathcal{M}_\bullet}{\sigma^2} \quad \approx 10^{-2} \left(\frac{\mathcal{M}_\bullet}{10^8 M_\odot}\right) \left(\frac{\sigma}{200\,\text{km}\,\text{s}^{-1}}\right)^{-2} \text{kpc}$$

linear scale of a typical galaxy

$$r_G \sim 10 - 100\,\text{kpc}$$

the direct dynamical influence of central SMBHs is relevant only in the innermost regions of the galaxies, and— due to the limited angular resolution of the optical telescopes — could be observable only in most massive galaxies located at distances <100 Mpc (effectively ~100 systems)

Andromeda (M31)

• relatively large angular size of the sphere of influence of the central SMBH

• small amount of gas, relatively young stars in the center, with older stars located at Keplerian orbits within the outer disk

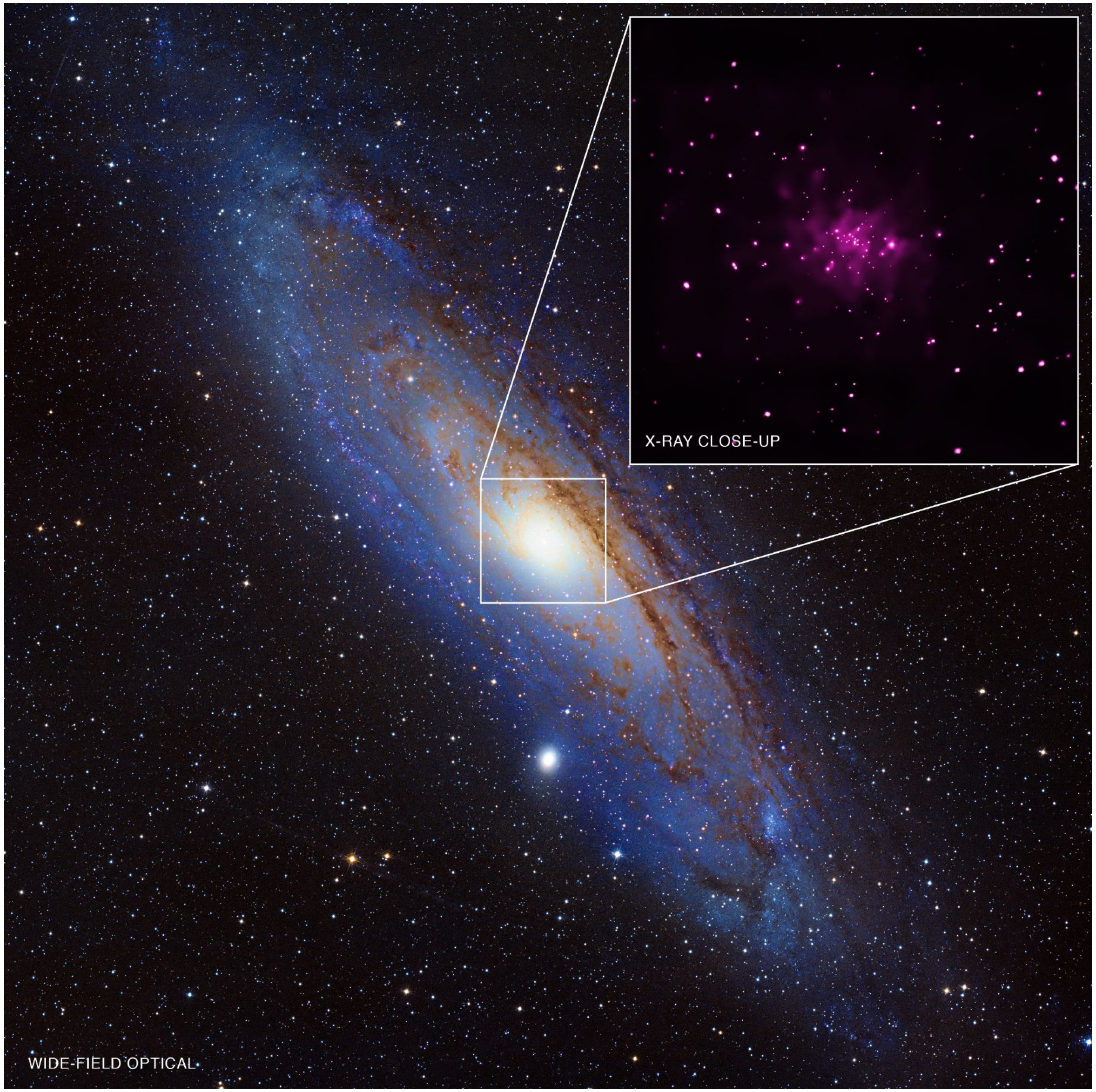

Andromeda (M31), distance 0.7 Mpc

radial velocities and velocity dispersion of the stars in the central parts of the galaxy gives **$M_\bullet$ = (1.1-2.3) x 10^8 $M_\odot$**

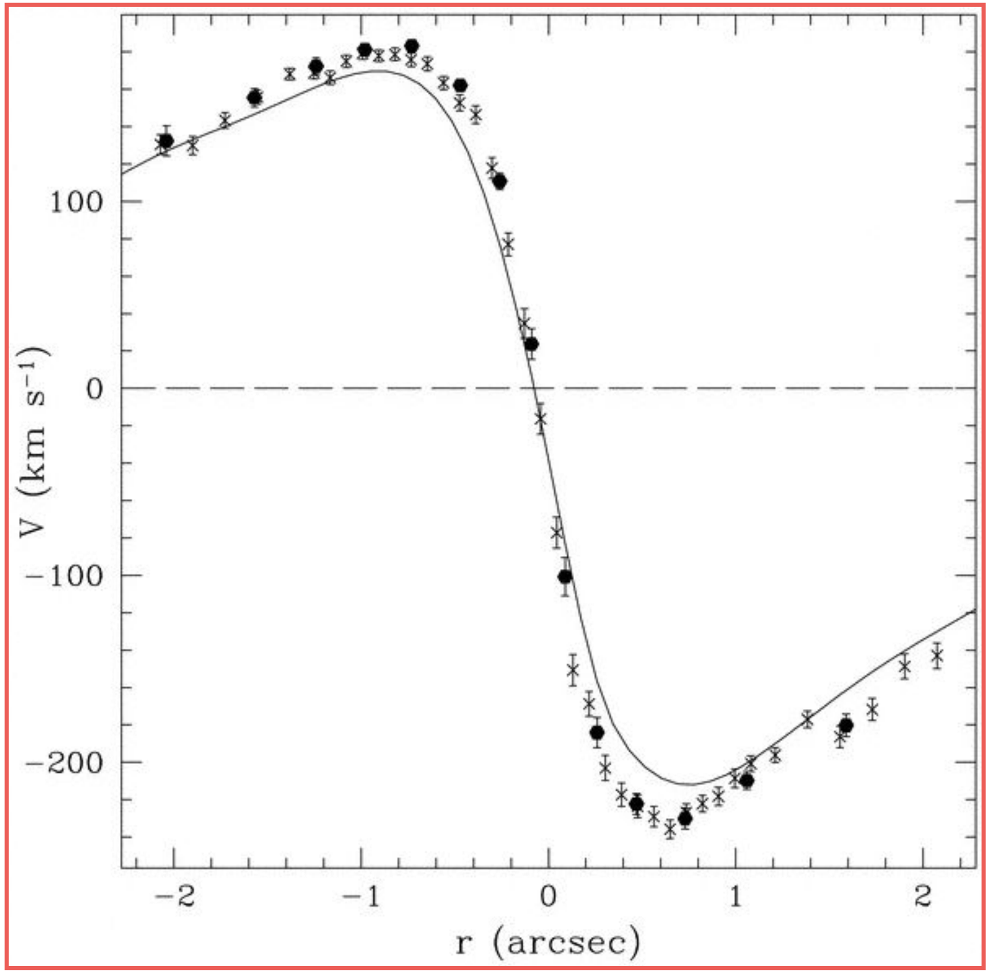

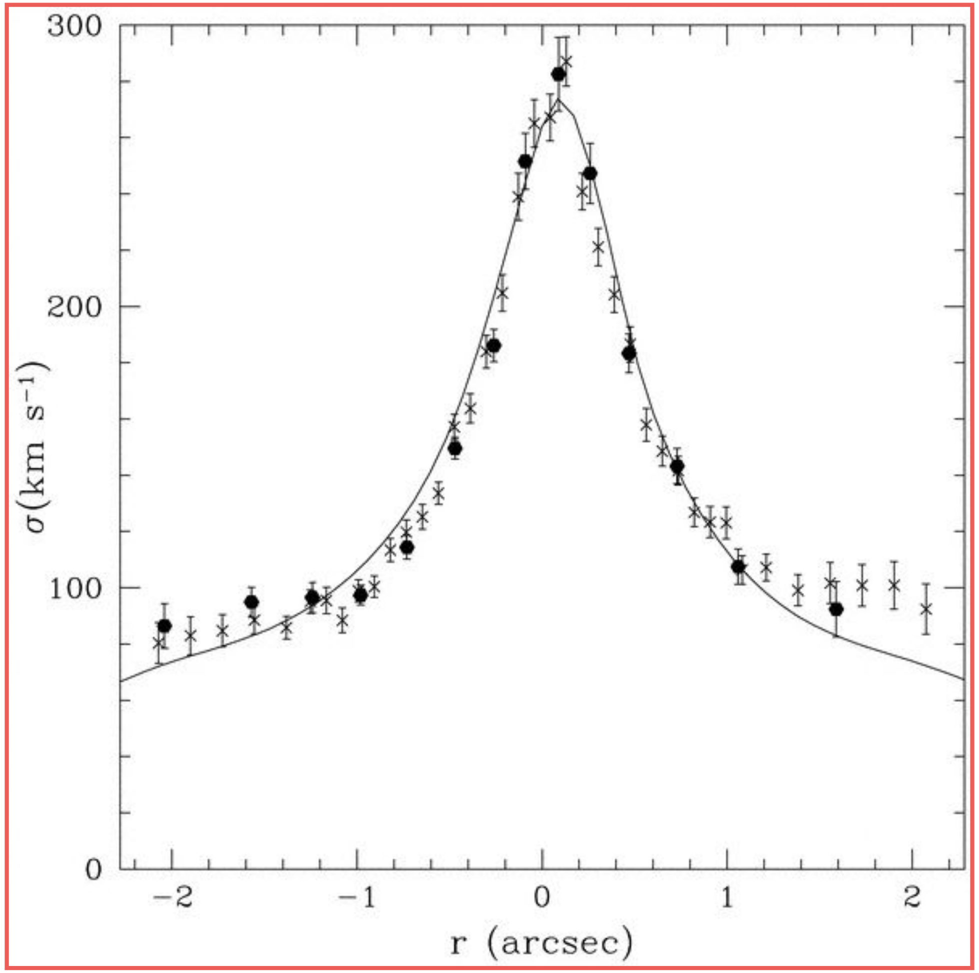

Peiris & Tremaine 2003

Bender et al. 2005

NGC 4258 (M106)
(X-ray – blue, Optical – gold, IR – red, Radio – purple)

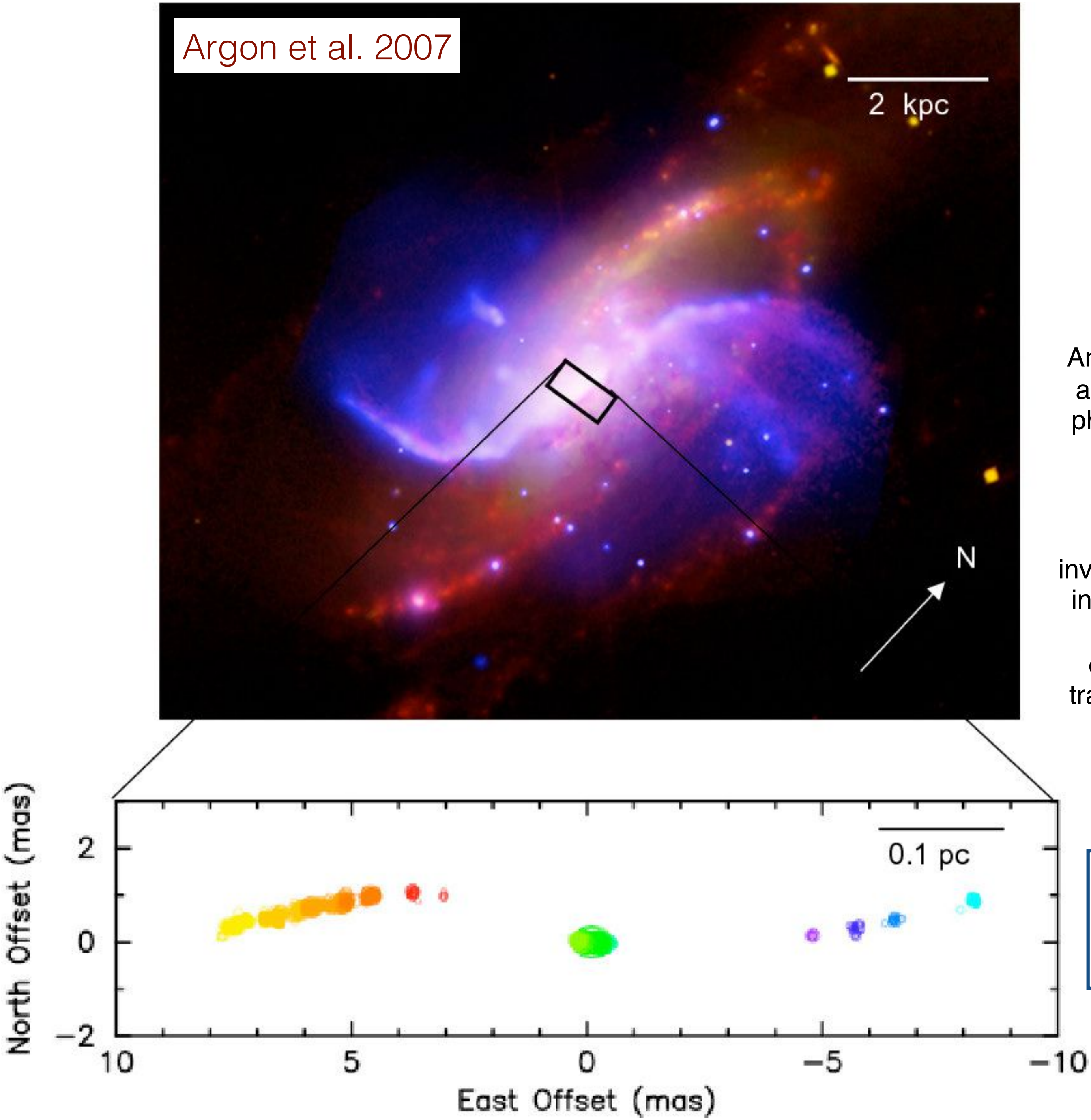

An atom or molecule may absorb a photon and move to a higher energy level, or the photon may stimulate emission of another photon of the same energy causing a transition to a lower energy level.

Producing a maser requires population inversion, i.e., a system with more members in a higher energy level relative to a lower energy level. Water maser emission is observed primarily at 22 GHz, due to a transition between rotational energy levels in the water molecule.

MASER = Microwave Amplification by Stimulated Emission of Radiation

NGC 4258, distance 7.6 Mpc

$$M_\bullet=(3.9\pm0.1)\times10^7\,M_\odot$$

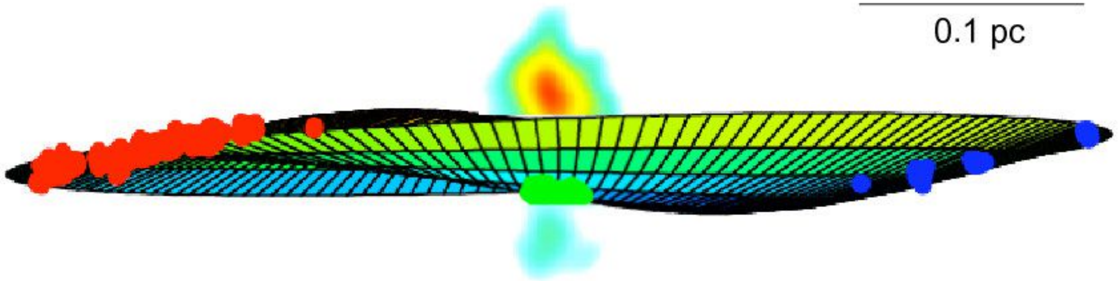

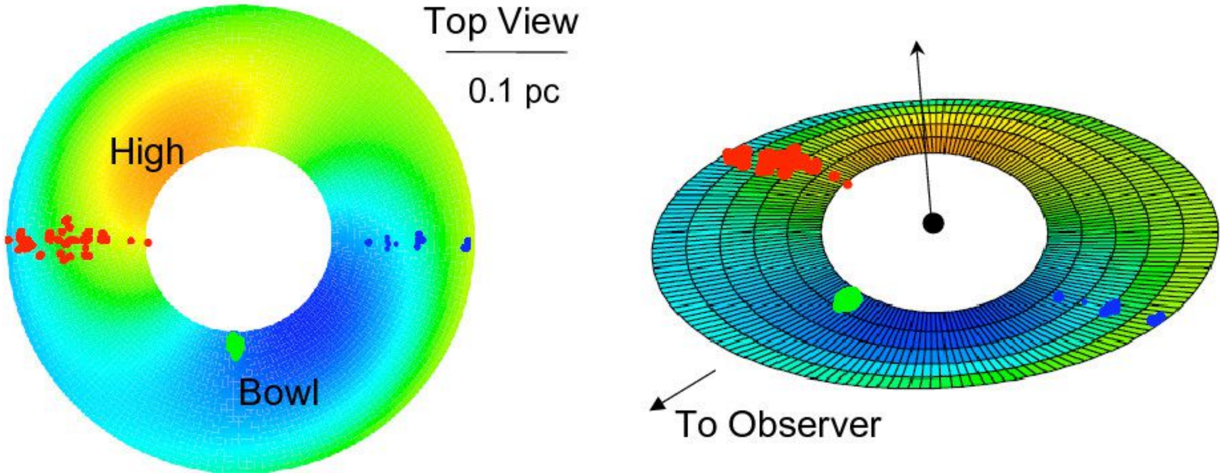

The phenomenon is observed in edge disks hosting molecular clouds with water molecules. The rest frame frequency of the maser line is 22 GHz and by measuring the Doppler shift due to the Keplerian motion of the clouds, the rotation curve of the disk can be measured, allowing the estimate of the BH mass.

Maser emission occurs only along the major axes (at 90deg with respect to the observer line of sight) of the edge on disk, and the nearest semi minor axis (if a photon at 22 GHz is emitted at an angle with respect to the observer, it encounters molecules with different radial velocities along the line of sight to the observer and Doppler shifts prevent maser amplification to occur).

Empirical **correlations** between the stellar velocity dispersion or the luminosity of a galaxy bulge and the mass of the central SMBH

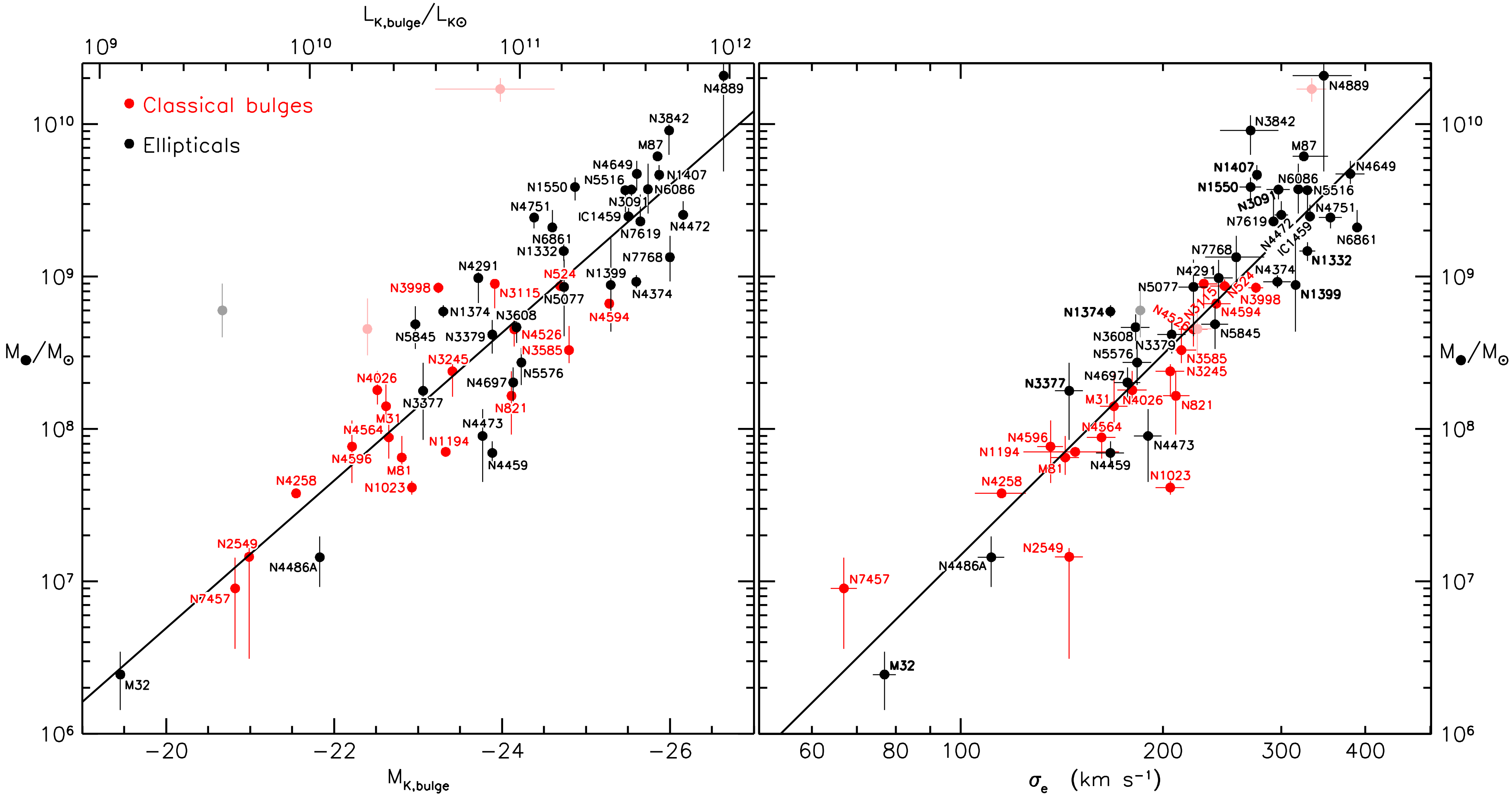

Kormendy & Ho 2013

Continuum and line emission in type I AGN

continuum: dominated by the innermost parts of the accretion disk, around the innermost stable circular orbit, i.e. a few/several r_S

broad emission lines: emitted from atomic gas in the “broad line region” (BLR), i.e. from dense clouds located at some distance from the central engine (but within the SMBH sphere of influence), and photoionized by the disk continuum

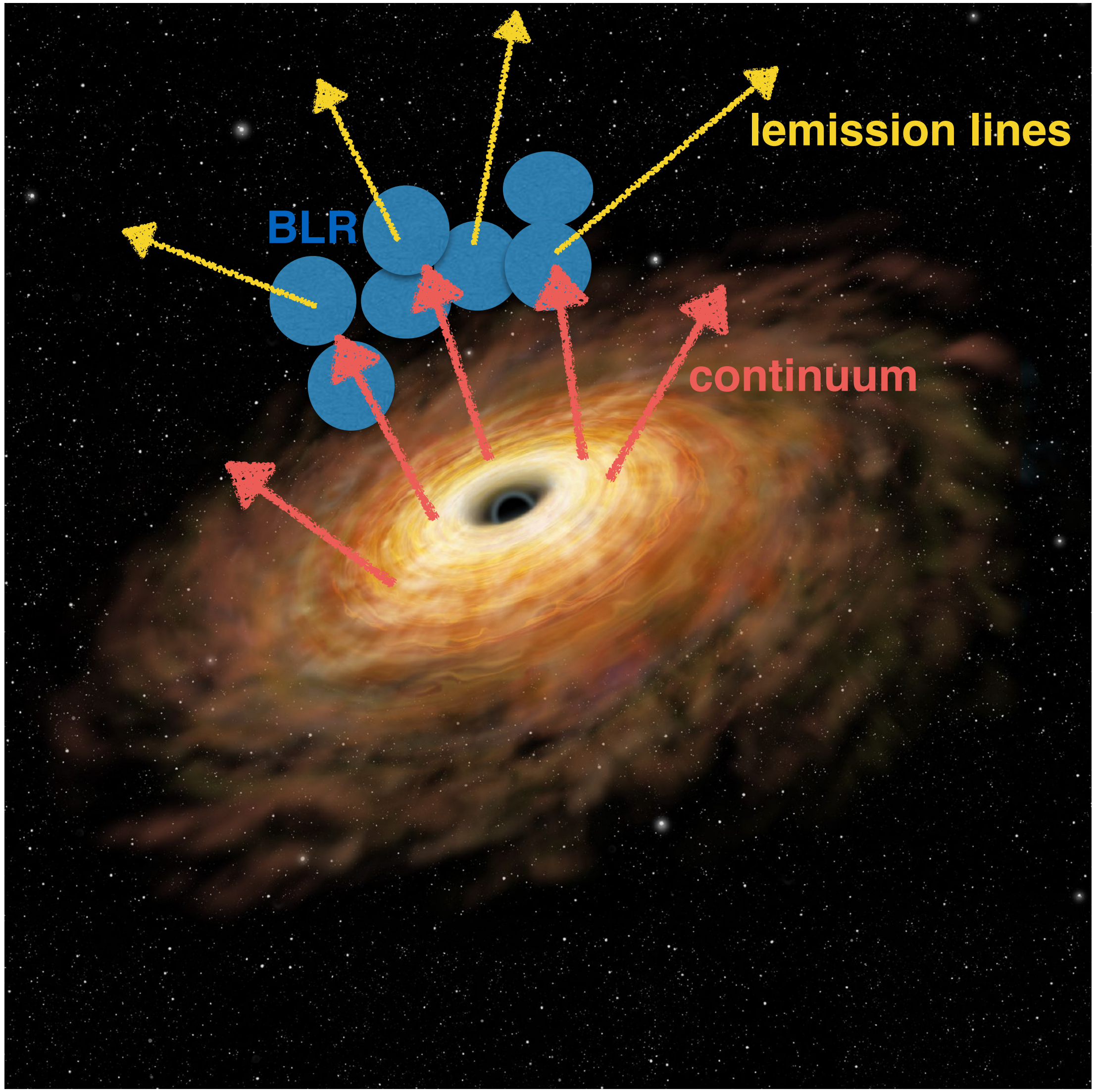

Reverberation mapping: the emission line variability shows a time lag with respect to the continuum — line intensity varies in response to the continuum variability, with a time lag Δt that can be associated to the distance of the BLR from the central engine via $R_{BLR} = c\Delta t$.

From the full width half maximum (FWHM) of the broad lines the velocity Δv of the gas can be inferred.

Main issues here: geometry and structure of the BLR!

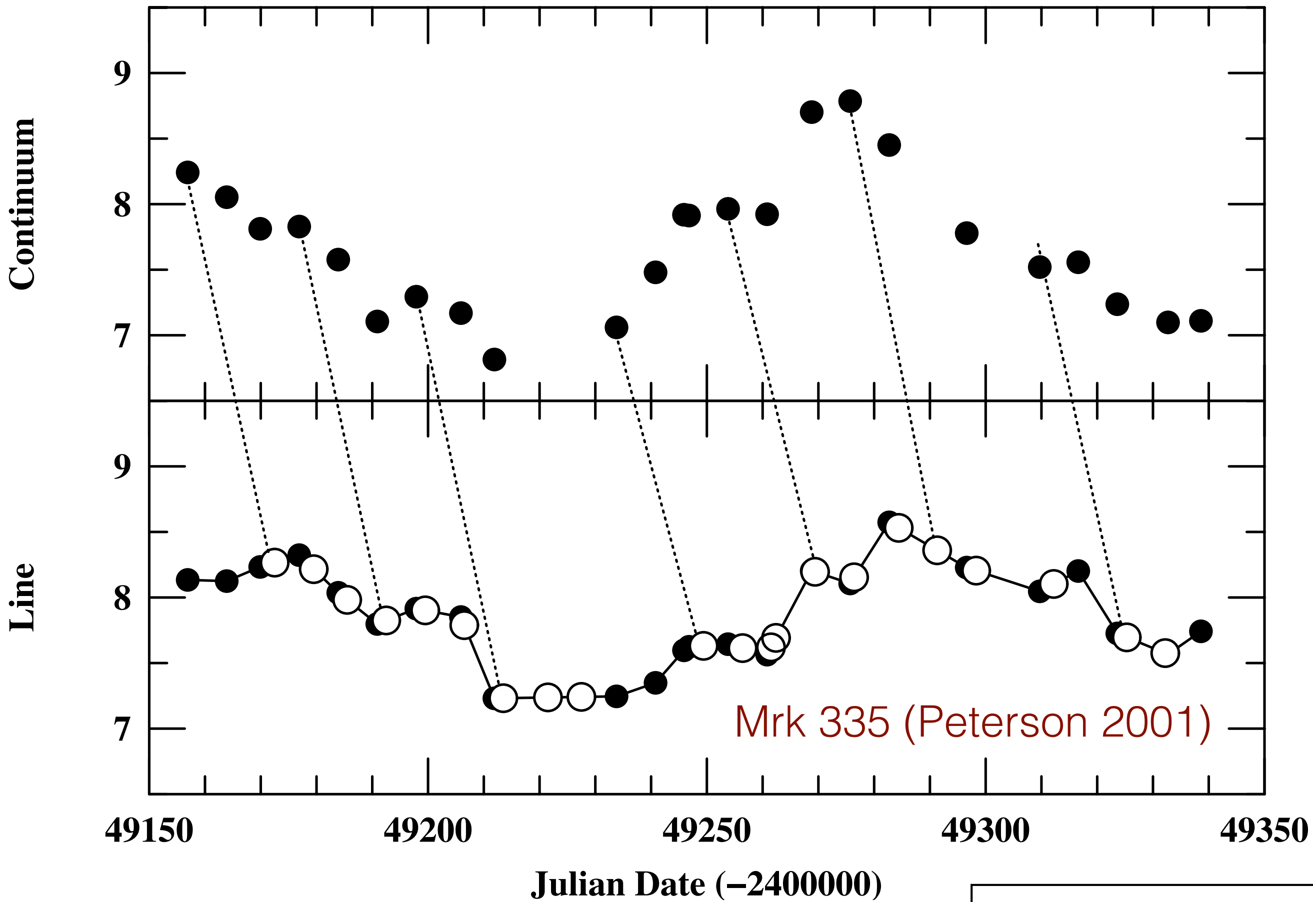

$$G\mathcal{M}_\bullet \sim R_{\rm BLR}\,(\Delta v)^2$$

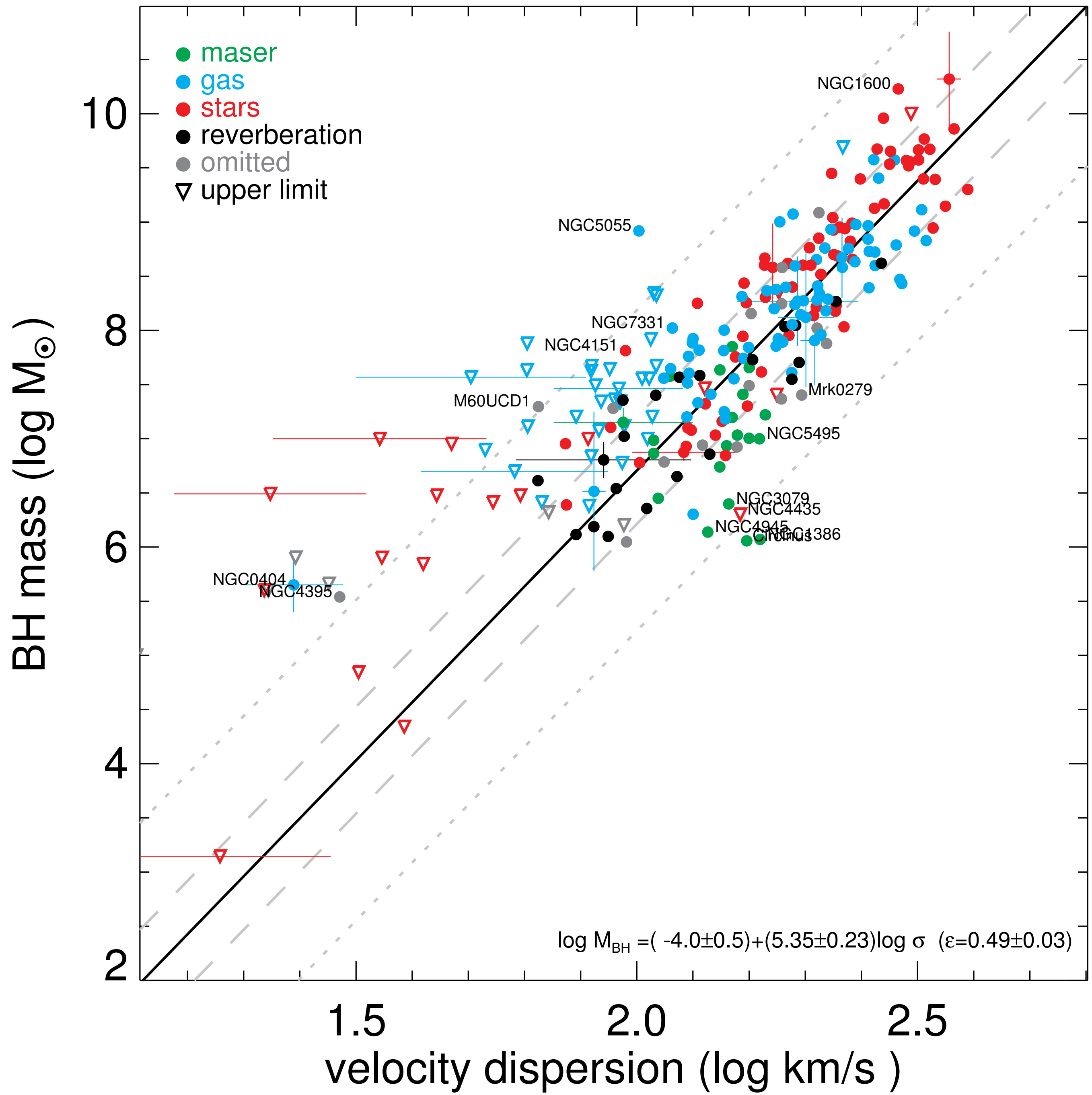

van den Bosch 2016

What if Δt cannot really be measure?

Empirical correlation between the characteristic broad-line region size R_{BLR} and the optical (continuum) AGN luminosity!

This relationship allows us to estimate R_{BLR} from the luminosity in a single AGN spectrum, thus by-passing the resource-intensive RM technique

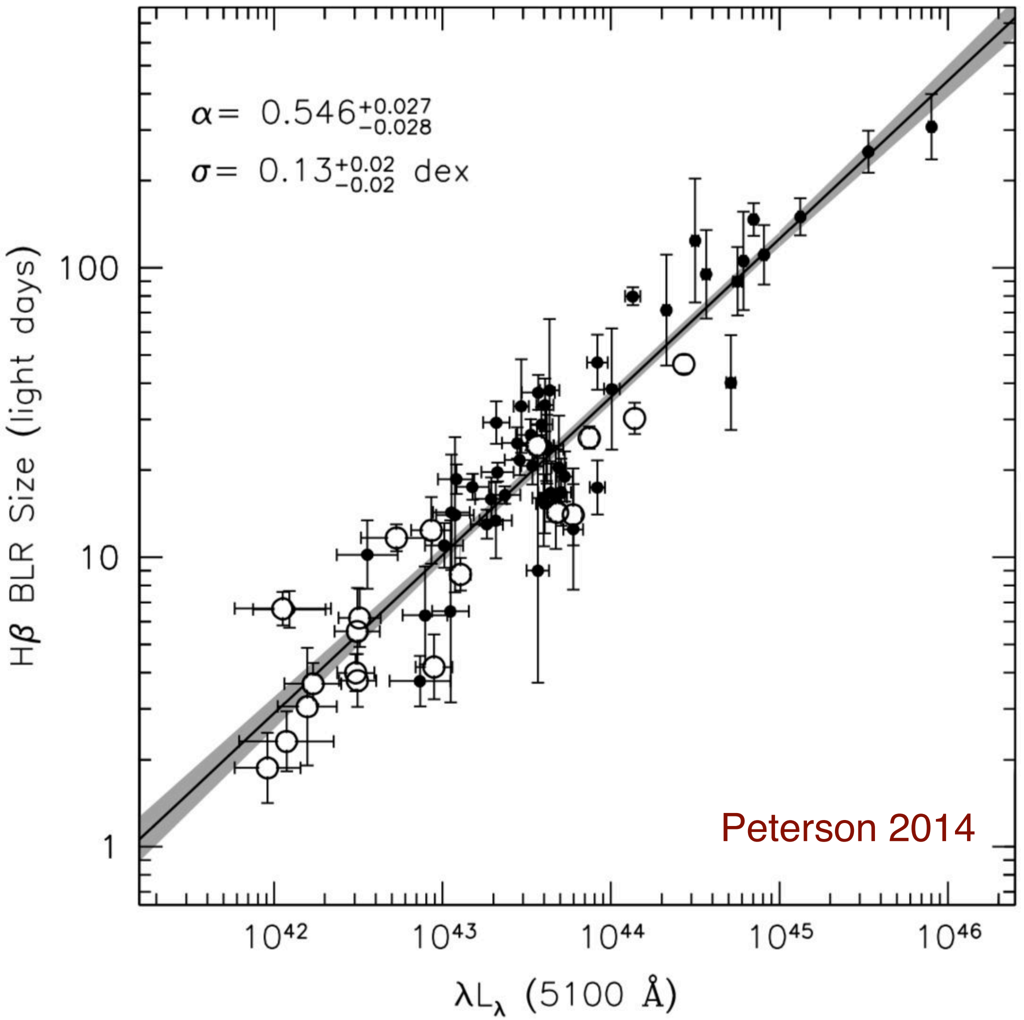

This single-epoch method is used for large samples of distant AGN using any of the prominent emission lines. The absolute mass uncertainty is evaluated statistically to be a factor ~4 to 5 on an absolute scale and a factor ~3 relative to the reverberation mapping-based mass. Individual mass estimates can be uncertain by a factor of ~10, however.

$$\log M_{\rm BH}({\rm H}\beta) = \log \left[\left(\frac{{\rm FWHM}({\rm H}\beta)}{1000 \ {\rm km \ s^{-1}}} \right)^2 \left(\frac{\lambda L_\lambda(5100\,\text{Å})}{10^{44}{\rm erg \ s^{-1}}} \right)^{0.50} \right] + (6.91 \pm 0.02)$$

e.g., Vestergaard & Peterson 2006

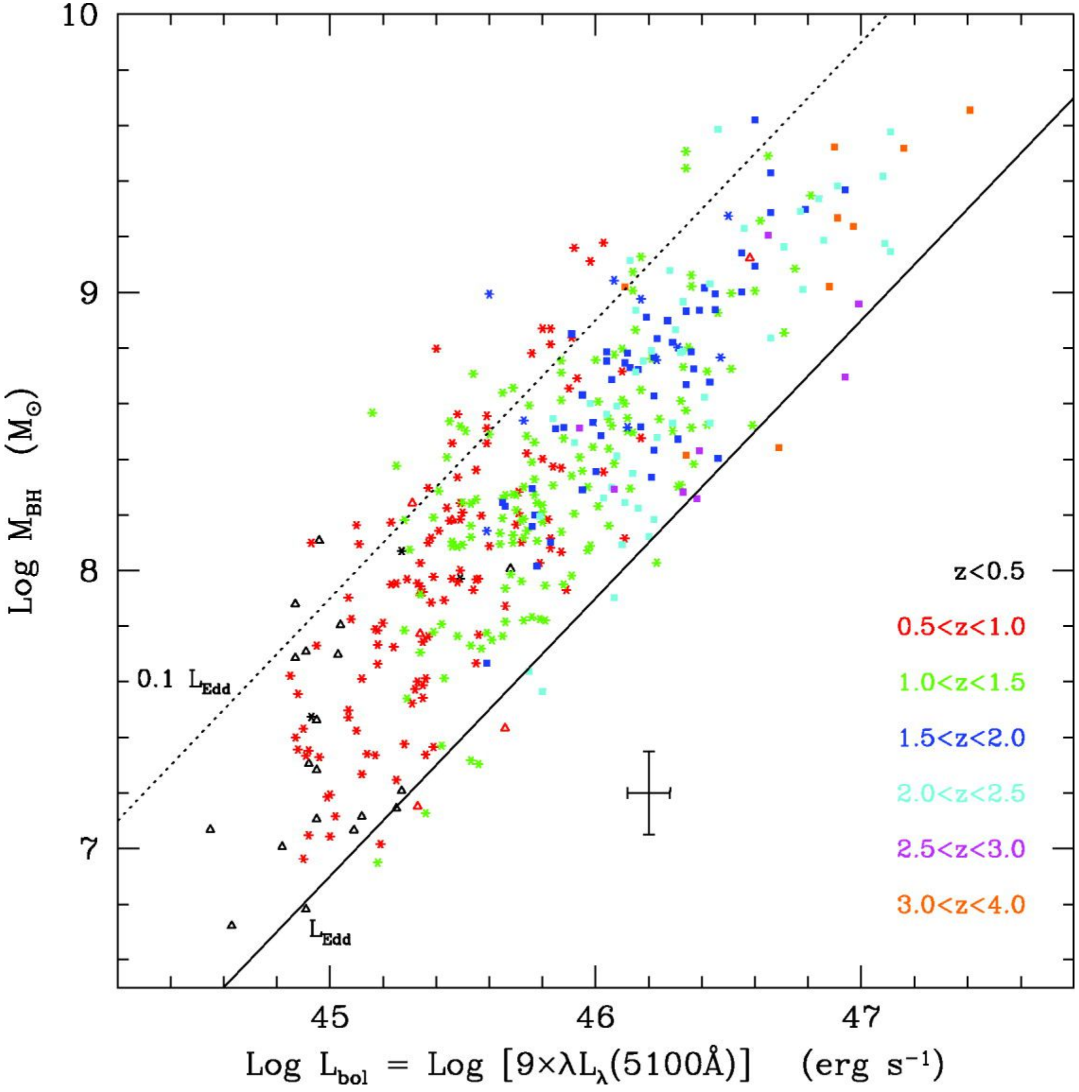

e.g., Kollmeier et al. 2006 (point types denote the emission line used for the mass measurement, with open triangles, asterisks, and filled squares corresponding to H-beta, Mg II, and C IV, respectively)

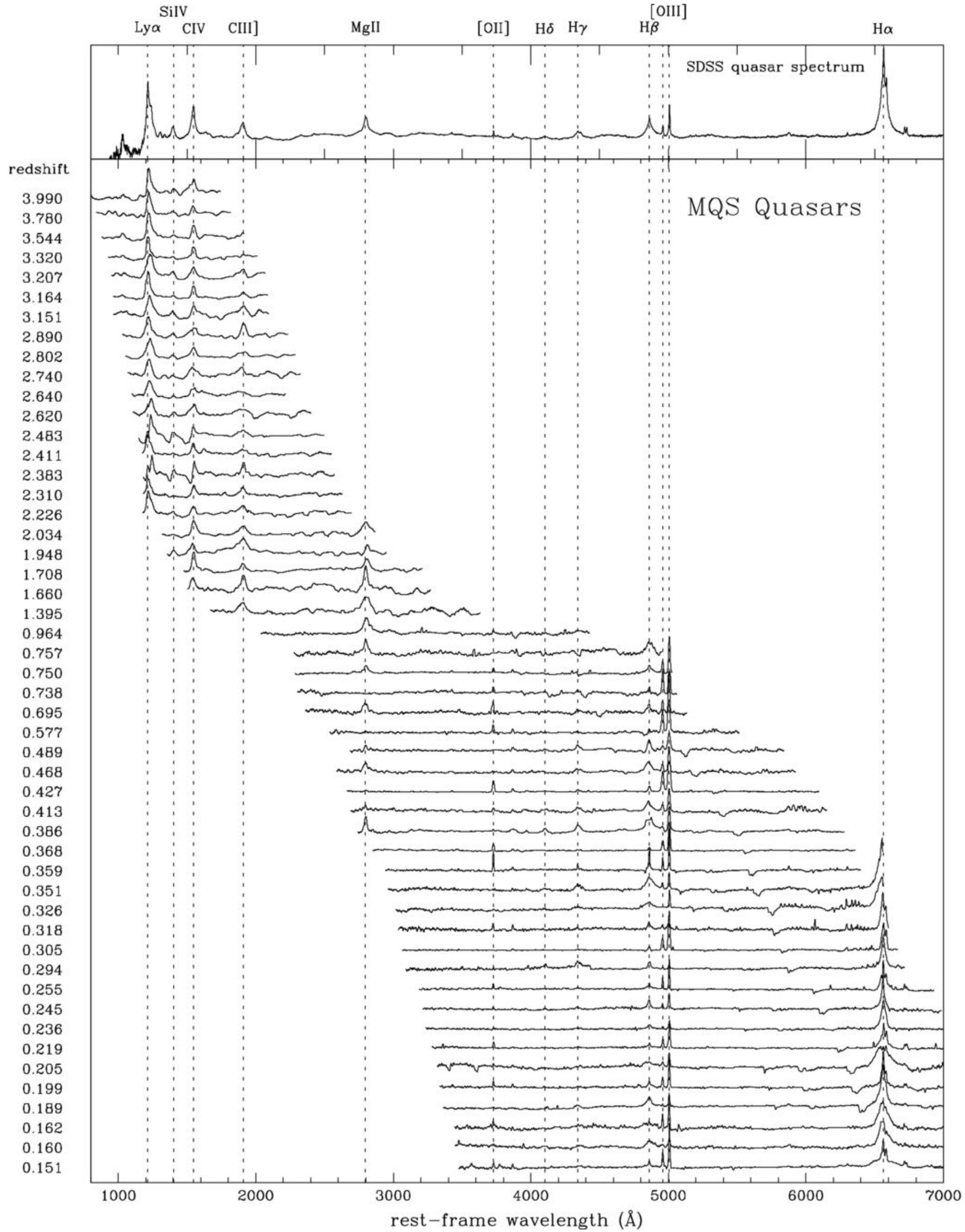

Kozlowski et al. 2013
spectroscopy of OGLE quasars

Active galaxies: accretion disks

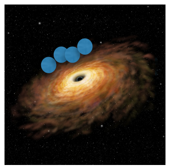

Active galaxies: accretion disks and dusty torii

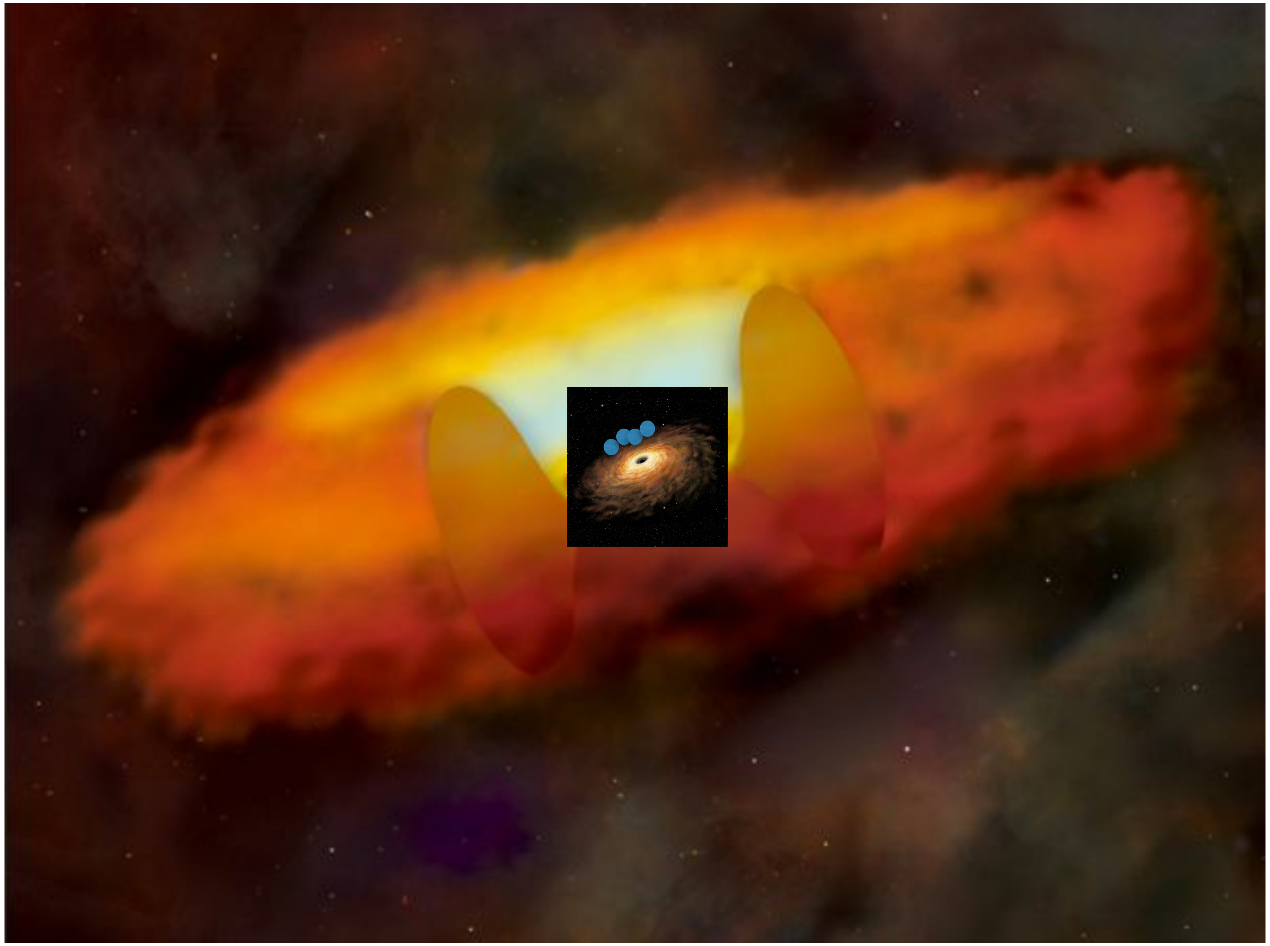

dusty torii in type 2 AGN may completely obscure central engines,
i.e. accretion disks and BLRs…

“Hidden” active galactic nuclei

X-ray spectroscopy

X-ray emission of accretion disk coronae

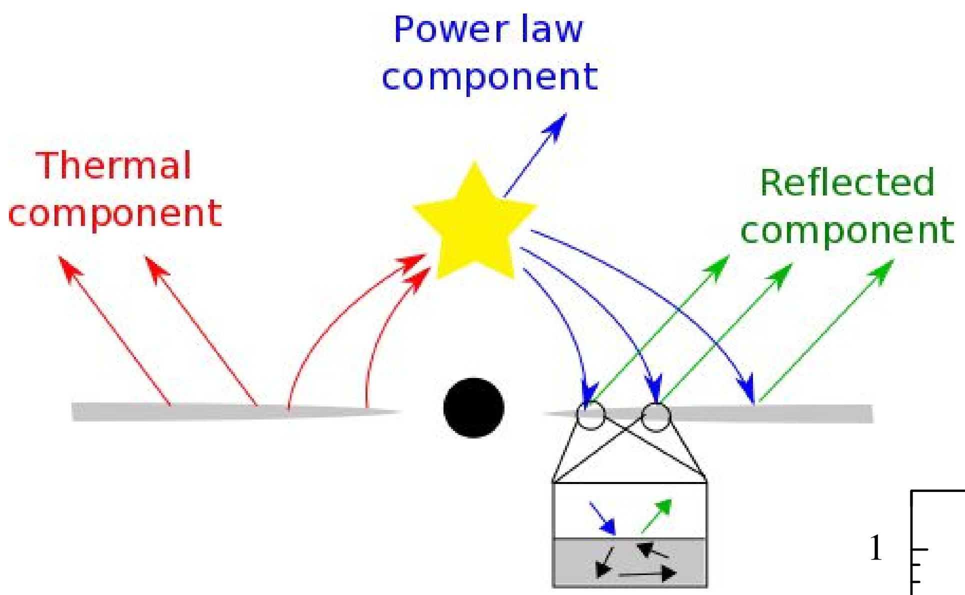

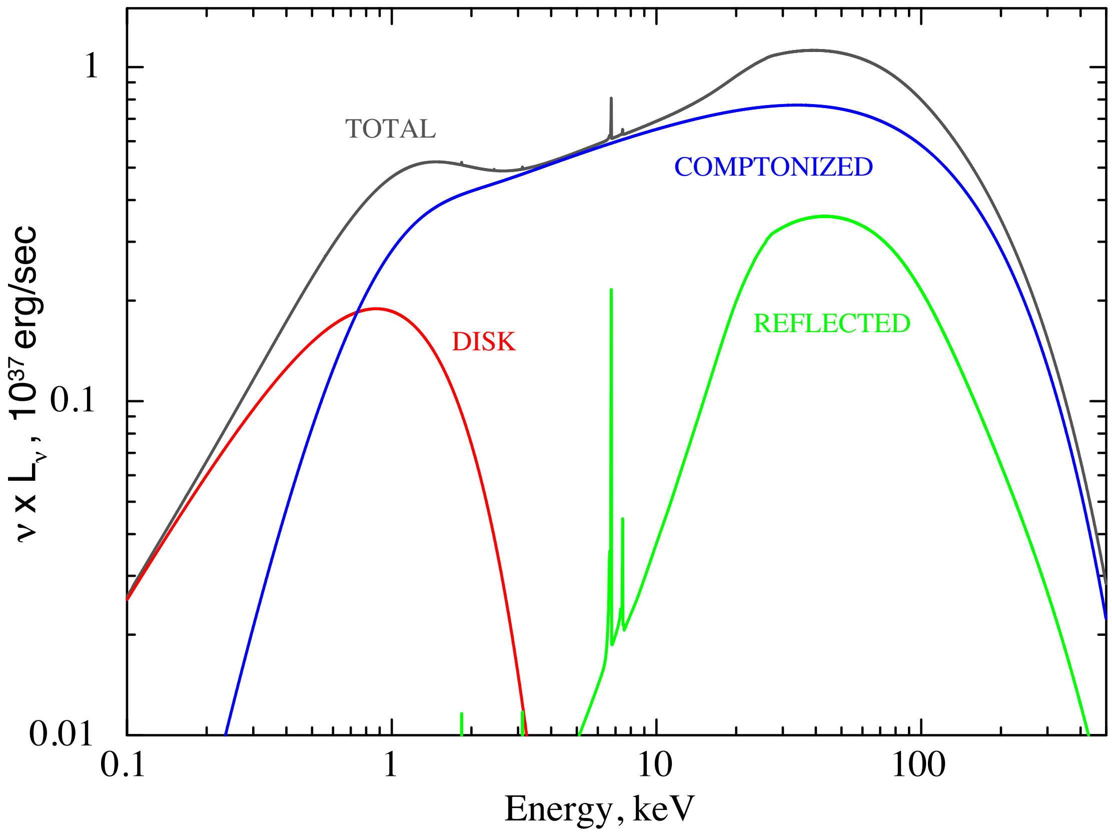

Bambi & Nampalliwar 2018

Spin measurements in BH XRBs

To date, there are three methods that have been widely applied in estimating the spins of stellar-mass BHs (Remillard & McClintock 2006), namely,

- **fitting the thermal continuum spectrum of the accretion disk,**
- **modeling the disk reflection spectrum with a focus on the Fe K line, and**
- **modeling high-frequency (~100–450 Hz) quasi-periodic oscillations (HFQPOs).**

While there are well-established models underpinning the first two methods, there is no agreed upon, or even leading, model of HFQPOs. Many classes of models have been proposed including several types of resonance models; global oscillation (“disko- seismic”) modes of the accretion disk; orbiting hot spots; tidal disruption of large inhomogeneities in the accretion flow; and the “relativistic precession” model.

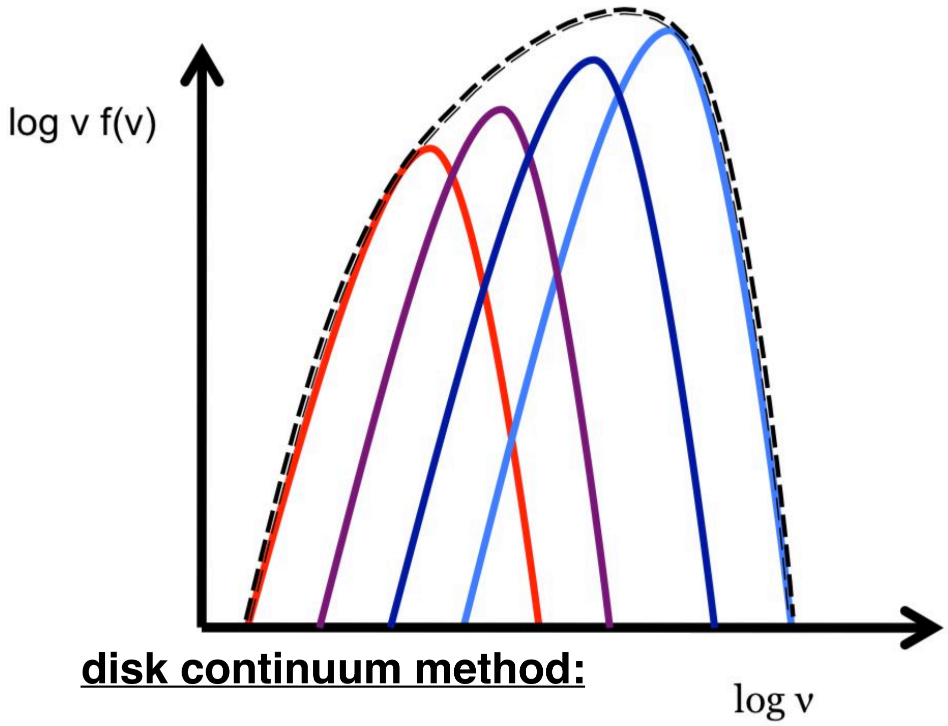

disk continuum method:

disk temperature depends on the radius, while at the same time the innermost stable circular orbit is a function of the BH spin: r_{isco} ~$6r_g$ for a=0, and ~r_g for a=1

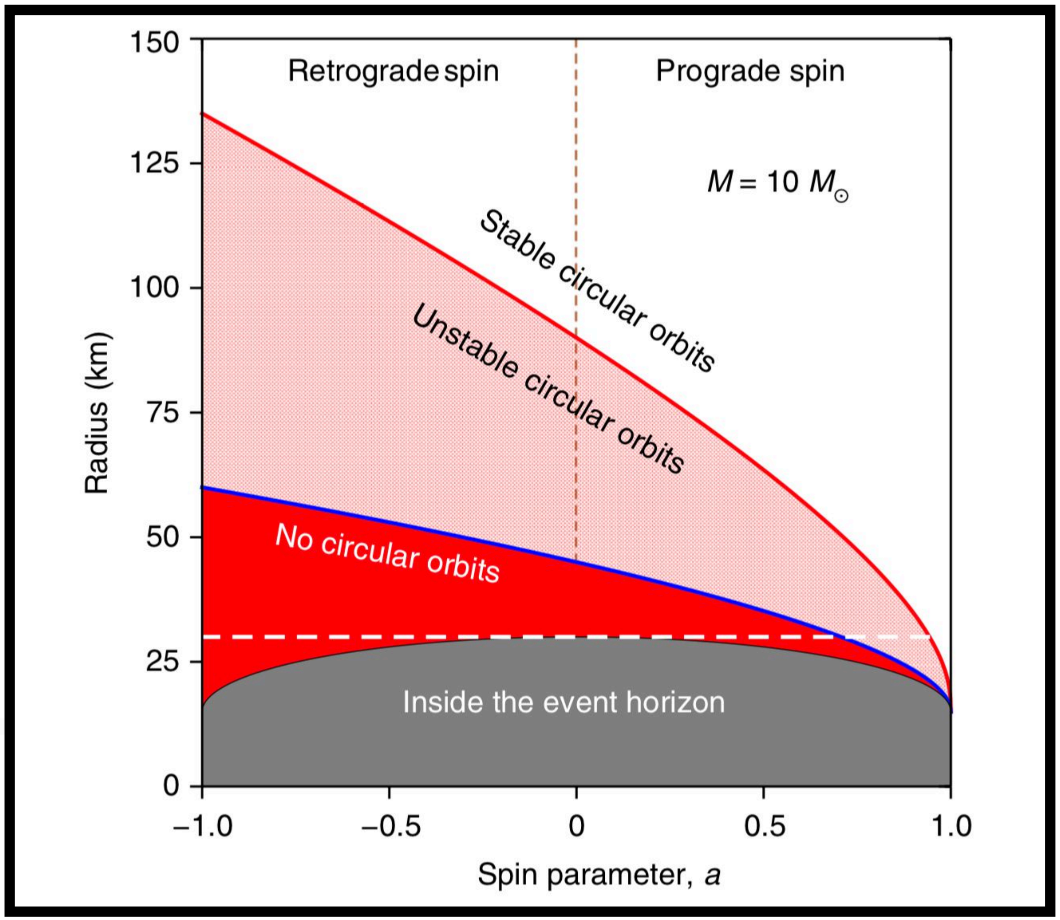

Reynolds 2019

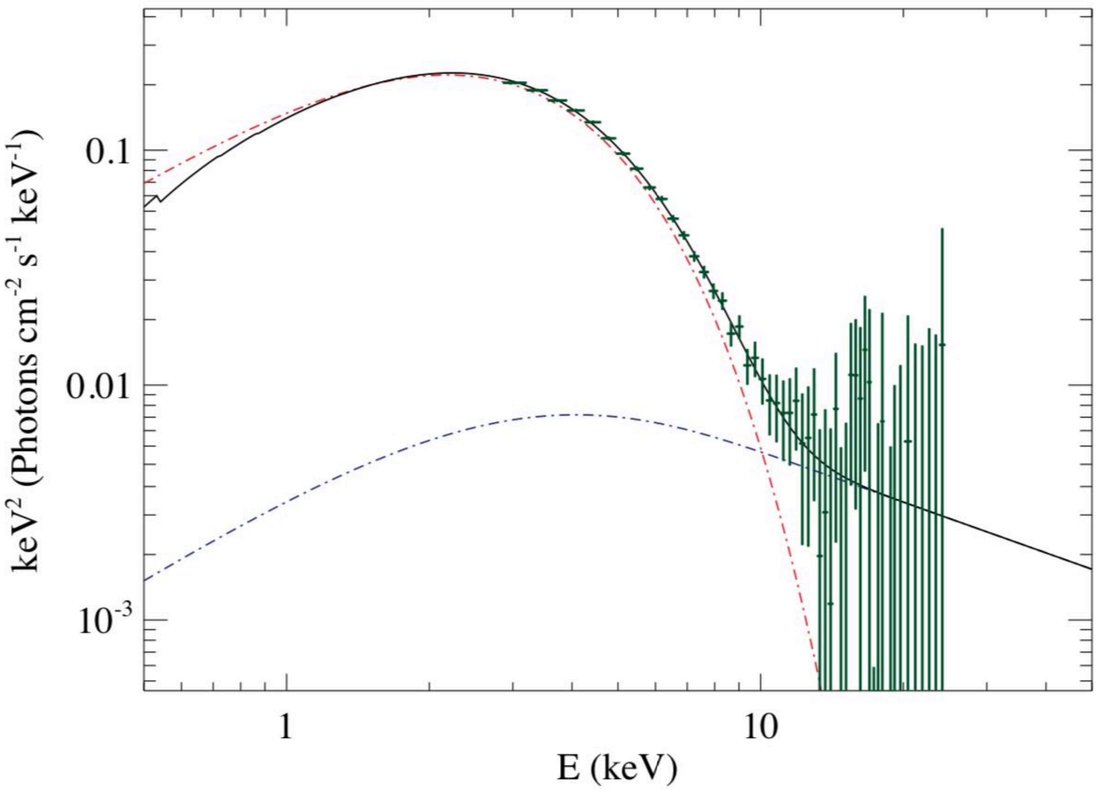

LMC X–3

Steiner et al. 2014

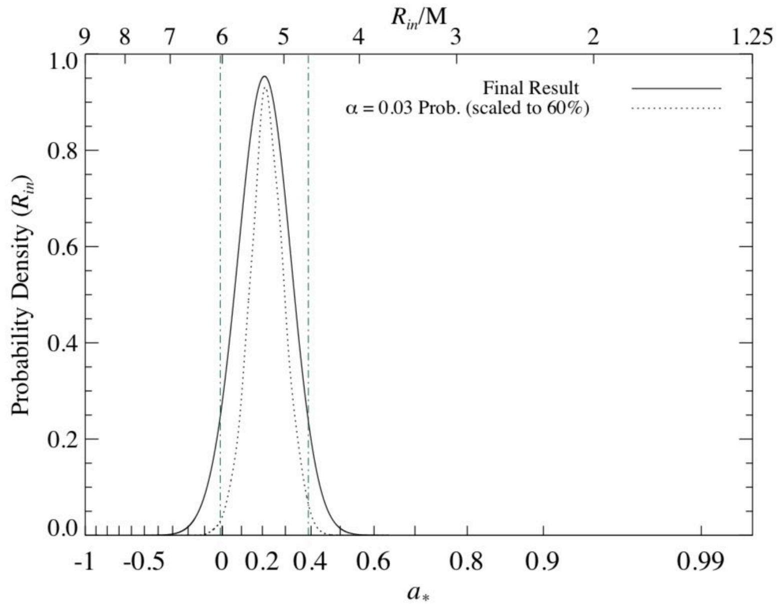

Method not applicable to AGN, as the BH mass estimates for AGN are much less accurate, and also the AGN disk continuum peaks at UV frequencies which are hardly accessible observationally

Fe: one of the most abundant heavy elements in the Universe, characterized in addition by a particularly high fluorescent yield (i.e. the probability that a photoelectric absorption event is followed by fluorescent line emission); the fluorescent line at ~6keV energies accessible for currently operating X-ray telescopes.

Newtonian

Special relativity

General relativity

Line profile

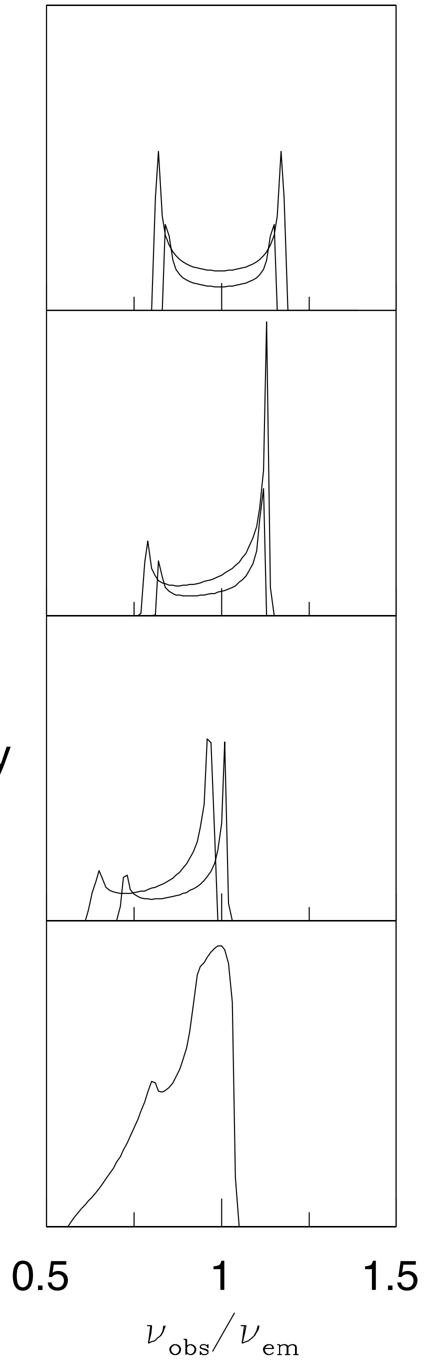

Transverse Doppler shift

Beaming

Gravitational redshift

Fabian 2013

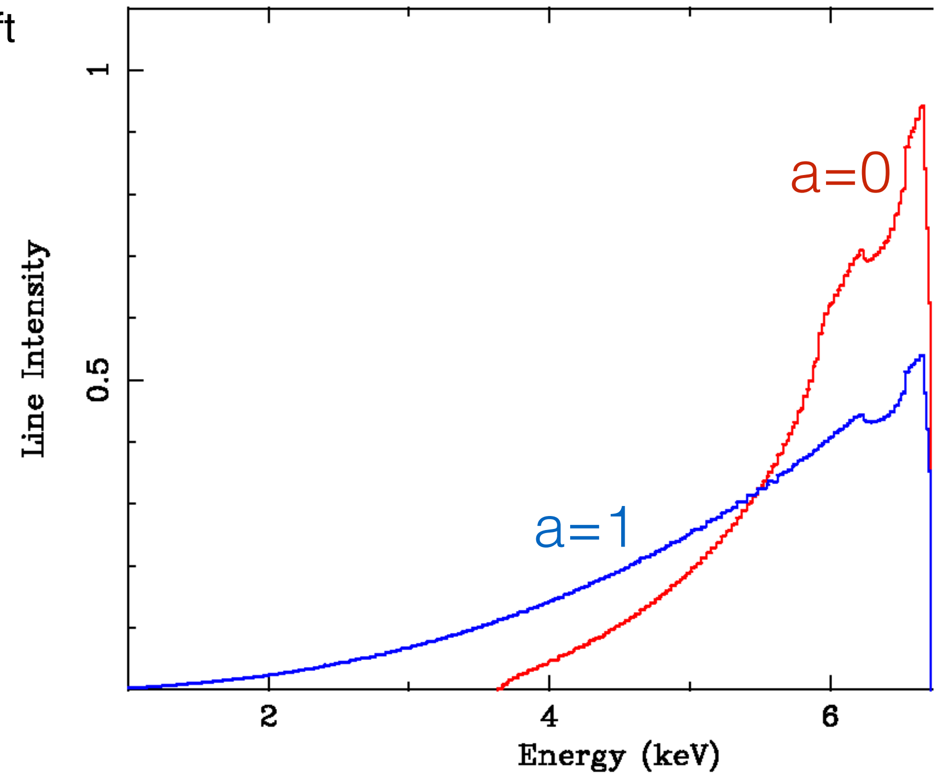

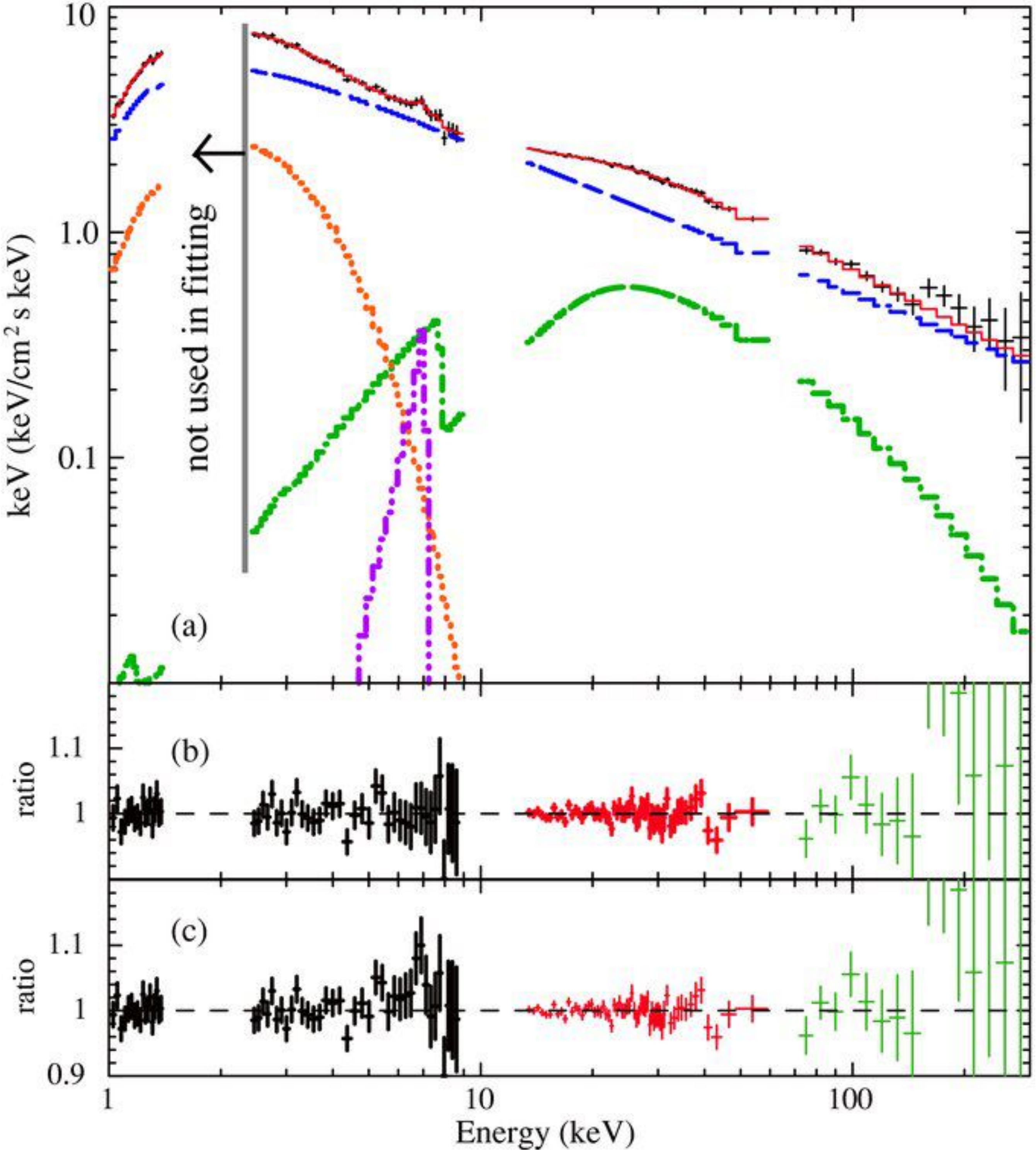

GX 339–4
Yamada et al. 2009

BH Binary	a_* (Continuum)	a_* (Iron)
GRS 1915+105	> 0.98	0.98 ± 0.01
Cygnus X-1	> 0.98	> 0.95
GS 1354-645	–	> 0.98
MAXI J1535-571	—	> 0.98
Swift J1658.2	—	> 0.96
LMC X-1	0.92 ± 0.06	$0.97^{+0.02}_{-0.25}$
GX 339-4	< 0.9	0.95 ± 0.03
XTE J1752-223	—	0.92 ± 0.06
MAXI J1836-194	—	0.88 ± 0.03
M33 X-7	0.84 ± 0.05	—
4U 1543-47	$0.80 \pm 0.10^{\star}$	—
IC10 X-1	$\gtrsim 0.7$	—
Swift J1753.5	—	$0.76^{+0.11}_{-0.15}$
XTE J1650-500	—	$0.84 \sim 0.98$
GRO J1655-40	$0.70 \pm 0.10^{\star}$	> 0.9
GS 1124-683	$0.63^{+0.16}_{-0.19}$	—
XTE J1652-453	—	< 0.5
XTE J1550-564	0.34 ± 0.28	$0.55^{+0.15}_{-0.22}$
LMC X-3	0.25 ± 0.15	—
H1743-322	0.2 ± 0.3	—
A0620-00	0.12 ± 0.19	—
XMMU J004243.6	< -0.2	—

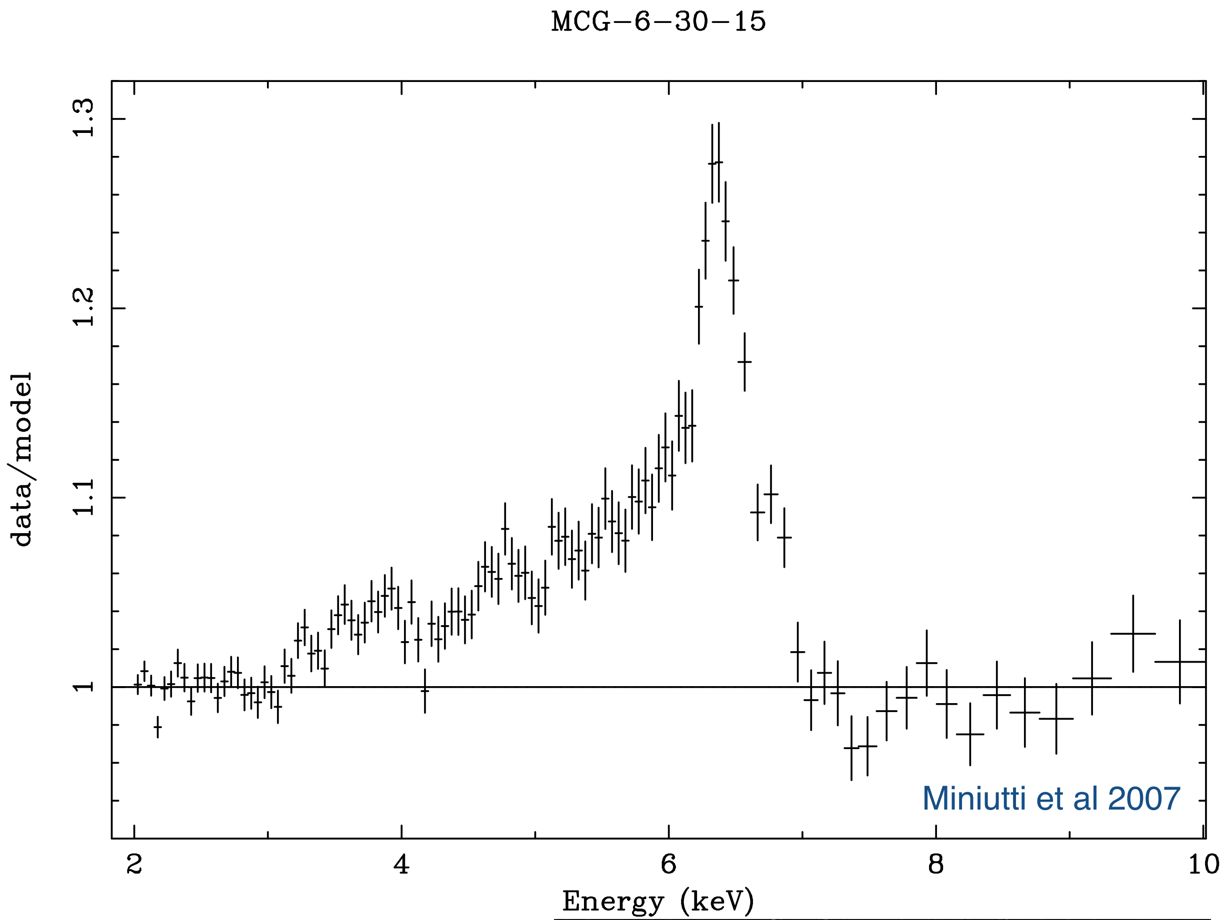

AGN

Object	a_* (Iron)
IRAS 13224-3809	> 0.99
Mrk 110	> 0.99
NGC 4051	> 0.99
1H0707-495	> 0.98
RBS 1124	> 0.98
NGC 3783	> 0.98
NGC 1365	$0.97^{+0.01}_{-0.04}$
Swift J0501-3239	> 0.96
PDS 456	> 0.96
Ark 564	$0.96^{+0.01}_{-0.06}$
3C120	> 0.95
Mrk 79	> 0.95
NGC 5506	$0.93^{+0.04}_{-0.04}$
MCG-6-30-15	$0.91^{+0.06}_{-0.07}$
Ton S180	$0.91^{+0.02}_{-0.09}$
1H0419-577	> 0.88
IRAS 00521-7054	> 0.84
Mrk 335	$0.83^{+0.10}_{-0.13}$
Ark 120	$0.81^{+0.10}_{-0.18}$
Swift J2127+5654	$0.6^{+0.2}_{-0.2}$
Mrk 841	> 0.56
Fairall 9	$0.52^{+0.19}_{-0.15}$

Accretion history of SMBHs (Soltan 1982)

Since the energy radiated away by a quasar after accreting the mass M_{acc} during the quasar lifetime is $\eta_d M_{acc} c^2 \sim \int dt\, L$, while at the same time the BH growth is $M_{BH} = (1-\eta_d) M_{acc}$, knowing the total electromagnetic energy density produced by quasars in the entire Universe (the X-ray background!), $U = \int dt \int dL\, L\, \Phi(L, z)$, and the mass density of SMBHs in the local Universe, ρ_{BH}, one may estimate the average radiative efficiency of the accreting matter, η_d, and hence the average BH spin for the quasar population: $\rho_{BH} c^2 = (1-\eta_d)\, U / \eta_d$

$\eta_d = 0.07$ non-rotating BH accreting at the Eddington rate ($a = 0$)

$\eta_d = 0.42$ maximally-rotating BH accreting at the Eddington rate ($a = 1$)

($\eta_d \ll 0.1$ for BH accreting at the sub-Eddington rate)

The luminosity function of quasars as a function of redshift, or equivalently the extragalactic background light, reflects the accretion history of local remnant SMBHs (Small & Blandford 1992).

Extragalactic Background Light

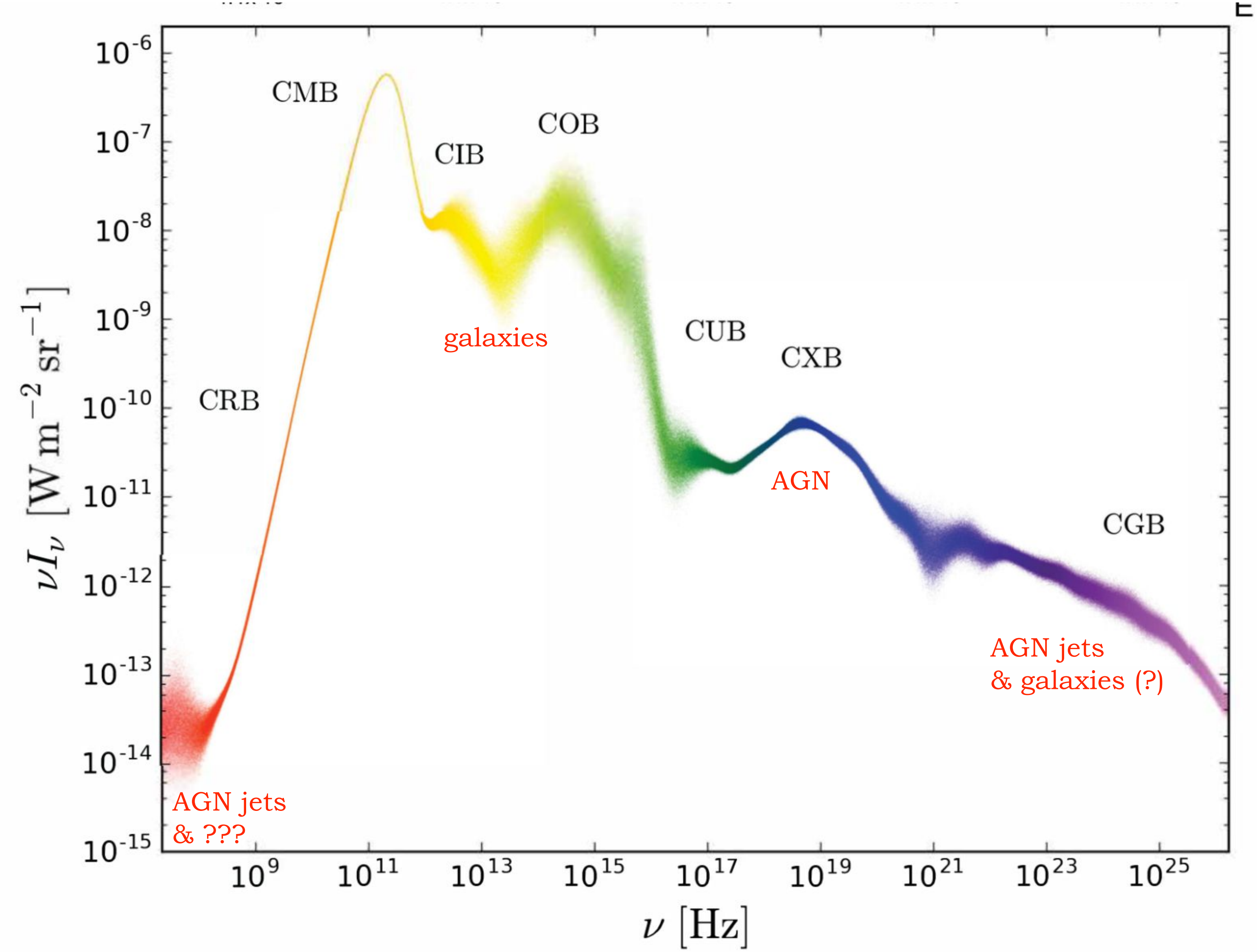

SMBH demographics

Graham & Driver 07

Study	Method	$\rho_{\rm bh,0}$ (E/S0) $10^5 M_\odot$ Mpc^{-3}	$\rho_{\rm bh,0}$ (Sp) $10^5 M_\odot$ Mpc^{-3}	$\rho_{\rm bh,0}$ (total) $10^5 M_\odot$ Mpc^{-3}
Graham et al. (2007)	$M_{\rm bh}$–n	$(3.46 \pm 1.16)h_{70}^3$	$(0.95 \pm 0.49)h_{70}^3$	$(4.41 \pm 1.67)h_{70}^3$
Wyithe (2006)	$M_{\rm bh}$–σ	...	...	$(1.98 \pm 0.38)h_{70}^3$
Fukugita & Peebles (2004)	$\rho_{\rm spheroid}$	$(3.4^{+3.4}_{-1.7})h_{70}$	$(1.7^{+1.7}_{-0.8})h_{70}$	$(5.1^{+3.8}_{-1.9})h_{70}$
Marconi et al. (2004)	$M_{\rm bh}$–(L, σ)	$3.3h_{70}^{0.74} f(h)$	$1.3h_{70}^{0.74} f(h)$	$(4.6^{+1.9}_{-1.4})h_{70}^{0.74} f(h)$
Shankar et al. (2004)	$M_{\rm bh}$–L	$(4.3^{+1.3}_{-1.1})h_{70}^{0.5} f(h)$	$(1.5^{+0.7}_{-0.7})h_{70}^{0.5} f(h)$	$(5.9^{+1.5}_{-1.5})h_{70}^{0.5} f(h)$
Shankar et al. (2004)	$M_{\rm bh}$–σ	$(3.4^{+1.1}_{-0.7})h_{70}^3$	$(1.4^{+0.5}_{-0.3})h_{70}^3$	$(4.8^{+1.2}_{-0.8})h_{70}^3$
McLure & Dunlop (2004)	$M_{\rm bh}$–L	$(4.8 \pm 0.7)h_{70}^{0.5} f(h)$	...	...
Wyithe & Loeb (2003)	$M_{\rm bh}$–σ	...	...	$(2.1^{+3.4}_{-1.3})h_{70}^3$
Aller & Richstone (2002)	$M_{\rm bh}$–σ	$(4.5 \pm 1.5)h_{70}^{0.39} f(h)$	$(1.4 \pm 1.3)h_{70}^{0.39} f(h)$	$(5.9 \pm 2.0)h_{70}^{0.39} f(h)$
Yu & Tremaine (2002)	$M_{\rm bh}$–σ	$(2.0 \pm 0.2)h_{70}^3$	$(0.9 \pm 0.2)h_{70}^3$	$(2.9 \pm 0.4)h_{70}^3$
Merritt & Ferrarese (2001)	$\rho_{\rm spheroid}$	...	...	$4.6h_{70}$
Salucci et al. (1999)	$\rho_{\rm spheroid}$	$6.2h_{70}^2$	$2.0h_{70}^2$	$8.2h_{70}^2$

Soltan (1982), Fabian and Iwasawa (1999), Elvis et al. (2002), Yu and Tremaine (2002), Marconi et al. (2004):

$\eta_d > 0.1$

Conclusions

Stellar-mass BHs:

BH masses in XRBs —
- orbital modulation (*companion star*)

BH spins in XRBs —
- accretion disk continua (*accretion disks*)
- Fe fluorescence lines (*disk coronae; X-ray reflection*)
- QPOs in accretion disk lightcurves ?

BH masses & spins in binary BHs —
- GW detections with LIGO/Virgo/KAGRA

SMBHs:

BH masses —
- individual stars (Sgr A*)
- stellar/gas velocity dispersion, maser emission (*nearby non-active galaxies*)
- reverberation mapping (*nearby type 1 AGN; geometry and structure of the BLR*)
- broad emission lines (*type 1 AGN; geometry and structure of the BLR*)

BH spin:
- Fe fluorescence line (*broad-band X-ray coverage with fine energy resolution*)
- CXB (*population; quasar luminosity function & cosmic background radiation*)

Stellar-mass BHs: mass distribution and binary merger rates?
IMBHs: where are they? how many?
SMBHs: change their masses and spins during cosmological co-evolution with host galaxies!

EHT: radio imaging of the event horizon in Sgr A* (and M87?)
ATHENA: broad-band X-ray spectroscopy with <10eV energy resolution (earlier: XRISM)
LISA: mergers of IMBHs and SMBH?

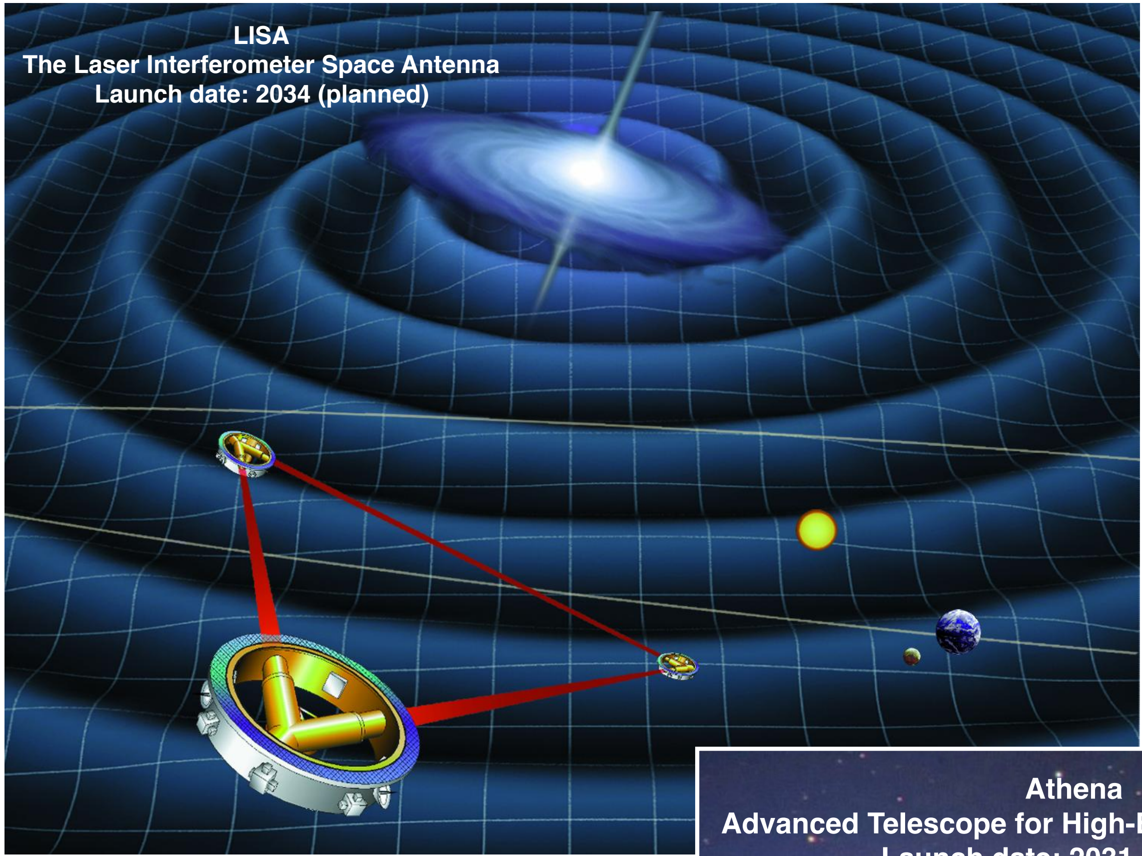
LISA
The Laser Interferometer Space Antenna
Launch date: 2034 (planned)

FUTURE

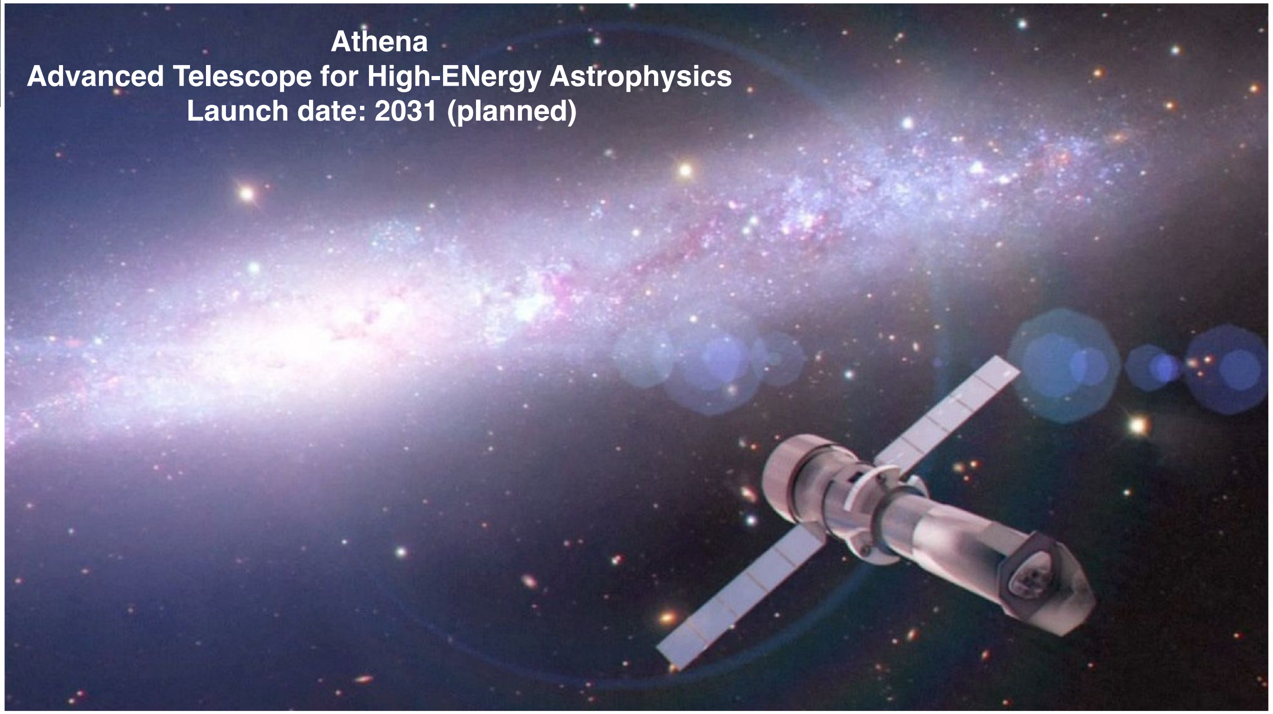
Athena
Advanced Telescope for High-ENergy Astrophysics
Launch date: 2031 (planned)